EUROPEAN COMMISSION
DIRECTORATE-GENERAL
Joint Research Centre

Bio-Optical Environmental Assessment of Marginal Seas

Progress Report 1

V. Barale [1], B. Weber [1,2], J.M. Jaquet [2]

[1] Institute for Environment and Sustainability
Joint Research Centre

[2] University of Geneva
Earth Sciences Section, Remote Sensing and GIS Unit

Collaboration Agreement Nº 21698-2004-02 SOSC ISP CH

2004 **EUR 21479 EN**

A great deal of additional information on the
European Union is available on the Internet.
It can be accessed through the Europa server
(http://europa.eu.int)

EUR 21479 EN

Printed in Italy

European Commission
Directorate-General Joint Research Centre
http://www.jrc.cec.eu.int

EUR 21479 EN
ISSN 1018-5593
Luxembourg: Office for Official Publications of the European Communities

Printed in Italy

Preface

The research described in the present report has been undertaken in the frame of Collaboration Agreement N. 21698-2004-02 S0SC ISP CH between the Institute for Environment and Sustainability (IES), Joint Research Centre (JRC) of the European Commission (EC), and the University of Geneva, Section of Earth Sciences, Remote Sensing and GIS Unit. The joint activities on Bio-optical Environmental Assessments of Marginal Seas were conducted at the JRC EC, within the FP6 Action 2121 ECOMAR, as part of Ms B. Weber's PhD Program at the University of Geneva.

Abstract

Optical remote sensing can highlight recurring and anomalous algal blooms in marginal and enclosed seas. The SeaWiFS-derived (1998-2003) database of chlorophyll-like pigment concentration (chl) was used to monitor algal growth in the Mediterranean basin. Yearly and monthly chl means were computed for the 6 years available, and climatological mean images derived. Then, interannual and seasonal variability was assessed computing yearly and monthly chl anomalies, as the difference between each individual year/month and the corresponding climatological year/month. The analysis of these anomalies provides a novel insight into the Mediterranean biological cycles, demonstrating algal blooms dynamics and related environmental boundary conditions.

Authors

V. Barale
Institute for Environment and Sustainability
Joint Research Centre of the European Commission
Via E. Fermi s.n. (tp 272), I-21020 Ispra (VA), Italy
Tel +39 0332 789274 Fax +39 0332 789034
e-mail: vittorio.barale@jrc.it

B. Weber
Remote Sensing and GIS Unit, Earth Sciences Section, University of Geneva
Rue des Maraichers 12, CH-1211, Switzerland
e-mail: barbara.weber@terre.unige.ch
and
Institute for Environment and Sustainability
Joint Research Centre of the European Commission
Via E. Fermi s.n. (tp 272), I-21020 Ispra (VA), Italy
e-mail: barbara.weber@jrc.it

J.M. Jaquet
Remote Sensing and GIS Unit, Earth Sciences Section, University of Geneva
Rue des Maraichers 12, CH-1211 Geneva, Switzerland
Tel +41 22 379 6615
e-mail: jean-michel.jaquet@terre.unige.ch
and
UNEP/DEWA/GRID, International Environment House
11 Chemin des Anémones, CH-1219 Châtelaine, Switzerland
e-mail : jean-michel.jaquet@grid.unep.ch

Reference

V. Barale, B. Weber and J.M. Jaquet (2004). Bio-optical Environmental Assessments of Marginal Seas. Progress Report 1. European Commission, EUR 21479 EN, pp. 50.

Table of Contents

Executive Summary

The research program on "Bio-optical Environmental Assessments of Marginal Seas" aims to exploit (optical) remote sensing to characterize eutrophic phenomena in the European Seas. Phytoplankton growth patterns can be assessed, at large (basin) scales and over long (seasonal and annual) periods, by means of systematic observations in the visible, which allow the determination of algal blooming markers such as chlorophyll-like pigments (*chl*). The analysis of the historical record of bio-optical satellite data, to monitor the concentration of *chl*, provides information on recurrent and/or anomalous algal blooms, and related environmental boundary conditions, to be used for the development of an indicator for (harmful) algal blooms.

Data collected by the SeaWiFS, in the period 1998-2003, have been used to explore the main features of the *chl* field in the Mediterranean Sea. The database was processed to correct for atmospheric errors and to derive *chl* values. In order to evaluate the background variability that could be found for the *chl* indicator, the first issue approached was a trend analysis of the SeaWiFS data set. Annual and monthly *chl* mean images were obtained for all available years, and then compared with the corresponding annual and monthly climatologies. The anomalies determined by this comparison were analysed in terms of the oceanographic climate of the basin. Climatologies derived from the data set collected by the CZCS, in the period 1978-1985, were used to provide an historical reference for the evaluation of the SeaWiFS imagery. The main features appearing in the SeaWiFS record are reminiscent of those already noted in the CZCS case. The SeaWiFS-derived *chl* values are quite consistent with the CZCS climatological means. The main differences appear in the northwestern (and westernmost) part of the basin, where more intense blooming seems to have occurred in the SeaWiFS period.

The assessment of interannual variability in the SeaWiFS data set was carried out by generating annual means of *chl* and then comparing each year with the climatological record. The *chl* anomalies at the annual scale were obtained as the difference between each individual year and the climatological year. The oligotrophic character of most sub-basins is the main feature of the Mediterranean Sea appearing in the climatological annual mean. The western and eastern basins are not dissimilar in the offshore domain, with an overall basin average of *chl* around 0.2 mg m^{-3}. The inshore domain presents higher *chl* values in the northwest and west, and lower *chl* values in the south and southeast. The features of the climatological annual mean image appear to be recurrent in the annual means. The average basin value of *chl* derived from the annual means shows a decrease on the order of 10% of the climatological average value for the entire basin. The *chl* annual anomalies highlight the geographical spread and intensity of blooming patterns, which differed in each year from the climatological

annual mean. The basin shows mostly positive anomalies in the first 3 years and mostly negative anomalies in the second 3 years.

The assessment of seasonal variability in the SeaWiFS data set was carried out by generating climatological monthly means of *chl* (*i.e.* 12 monthly means obtained as the average of the 6 realizations available for each month in the period 1998-2003), and then comparing single monthly means with the climatological record. A time component was coupled to the evaluation of space patterns, by computing the monthly sequence of *chl* anomalies, as the difference between each individual month and the corresponding climatological month. The spatial patterns in the climatological monthly means are not dissimilar from those observed at the annual scale, but show enhancements over (variable) seasonal periods. The SeaWiFS-derived time series presents a seasonal cycle of *chl* analogous to the one appearing in the historical CZCS data set, *i.e.* a bimodal pattern with *maxima* in the colder season, from late fall to early spring, followed by *minima* in the warmer one, from late spring to early fall. This is evident in the fluctuations of the average basin value of *chl* derived from the monthly means (*i.e.* a single *chl* value computed as the total average of all pixels composing each monthly image). As noted already for the annual means, the *chl* indicator displays a decreasing trend, over the period of SeaWiFS coverage, on the order of 20% of the climatological average value for the entire basin.

The climatological seasonal trend, obtained computing an average basin value of the *chl* indicator from the climatological monthly mean images, confirms for the Mediterranean Sea a behaviour similar to that of a sub-tropical basin, where the light level is never a limiting factor (so that its decrease in winter does not inhibit algal growth), but the nutrient level always is. Unlike what is seen in the historical CZCS data set, though, the climatological seasonal cycle in the SeaWiFS-derived time series shows that *chl*, after the summer low, grows systematically in fall, only to reach its absolute *maximum* in the middle of winter and then decrease rapidly in spring, toward its summer *minimum* again. This does not affect the general validity of the sub-tropical scenario, but points to the fact that some regions, namely the western sub-basins, have a somewhat different seasonality, so pronounced that it affects basin statistics, when integrated *chl* values are considered to summarize the behaviour of the basin as a whole.

The analysis of SeaWiFS-derived *chl* anomalies provides a novel insight into the space and time patterns of biological cycles in the Mediterranean Sea, demonstrating algal blooms dynamics and related environmental boundary conditions. Future activities include an in-depth analysis of both the *chl* monthly mean record and the sequence of monthly anomalies computed on the basis of the climatological data record, as well as the development of a “bloom anomaly algorithm” designed to detect short-term (albeit also recurring) events.

1. Introduction

Broad theme of the research program on "Bio-optical Environmental Assessments of Marginal Seas" is the exploitation of (optical) remote sensing data for the environmental assessment of the European Seas. The planned activities focus on the appraisal of recurring and/or anomalous phytoplankton growth patterns in enclosed seas – in the Mediterranean basin, in a first phase, and then in the other continental basins – with implications ranging from water quality to climate issues. The final goal is to characterize eutrophic phenomena in surface waters, monitoring the concentration of chlorophyll-like pigments (*chl*), as appearing in the historical record of bio-optical satellite data, to develop an indicator of (harmful) algal blooms.

Phytoplankton growth patterns can be assessed, at large (basin) scales and over long (seasonal and annual) periods, by means of systematic observations in the visible spectral range, which allow the determination of algal blooming markers such as *chl* (see Barale, 1994, and references therein). In near-coastal waters, significant uncertainties can arise in the computation of *chl* absolute values, due to the presence of other optically active materials (*i.e.* dissolved organic matter and suspended inorganic particles). Nevertheless, the analysis of historical times of satellite data can provide information on recurrent and/or anomalous algal blooms, and related environmental boundary conditions (Barale and Schlittenhard, 1994).

In this report, data collected by the Sea-viewing Wide Field-of-View Sensor (SeaWiFS), in the period 1998-2003, will be used to explore the large-scale, long-term features of the *chl* field in the Mediterranean Sea. In order to understand the degree of background variability that could be found for this indicator – background variability on which anomalies could appear to be superimposed – the first issue approached was a trend analysis of the SeaWiFS data set at hand. Annual and monthly *chl* mean images were obtained for all available years, and then compared with the corresponding annual and monthly climatologies. The anomalies determined by this comparison will be discussed in terms of the oceanographic climate of the basin.

1.1 Historical Data Records

At this time, sizeable times series of historical bio-optical data collected from satellite have been generated only by the *Coastal Zone Color Scanner* (CZCS), from November 1978 to May 1986, and by the *Sea-viewing Wide Field-of-View Sensor* (SeaWiFS), from September 1997 to present. Other orbital sensors that operated in the past, like the *Moderate Optoelectrical Scanner* (MOS), did not have the wide swath needed to ensure quasi-daily coverage of the Earth's surface, or had short-lived (less than 1 year long) missions, like the *Ocean Color and Temperature Scanner* (OCTS), the *Global Imager* (GLI), and the

sensors devoted to assess *POLarization and Directionality of the Earth's Reflectances* (POLDER, I and II), failing to provide full seasonal coverage of the oceans. New sensors, like the *Moderate Resolution Imaging Spectroradiometer* (MODIS), *Terra* and *Aqua* versions, and the *MEdium Resolution Imaging Spectrometer* (MERIS), are currently generating time series of bio-optical data, but these are not yet comparable to those of the CZCS and the SeaWiFS.

The historical data record generated by the CZCS mission has been used in several studies for an analysis of phytoplankton dynamics in the Mediterranean Sea. Examples of basin-scale assessments are provided by Morel and André (1991) and by Antoine et al. (1995), who looked at algal biomass and primary production in the western and eastern Mediterranean, respectively. Regional assessments have been conducted also for selected sub-basins, characterized by peculiar spatial and/or seasonal variations in the *chl* field, such as the Adriatic Sea (*e.g.* Barale *et al.*, 1986), the Alboran Sea (*e.g.* Arnone *et al.*, 1990), the Levantine sub-basins (*e.g.* Gitelson *et al.*, 1996). More recently, Barale (2003) summarized the indications coming from the CZCS-derived climatological data, for a comparison with other satellite data on sea surface temperature and wind speed, collected over the entire Mediterranean Sea during the last two decades.

The CZCS climatological *chl* record (1979-1985) for the Mediterranean Sea, obtained by the Ocean Colour European Archive Network (OCEAN) Project (see Barale et al., 1999, and Sturm et al., 1999, for a detailed description of the data set and of the algorithms used to generate it), is shown in the Plates 1, 2 and 3. Annual means are not shown for 1978 and 1986, when data were collected by CZCS only for the last three and first four months of the year, respectively. The annual mean of 1985 is also excluded, due to the fact that data collection was rather poor, during that year, except for the summer season. Therefore the yearly statistics are not directly comparable with those of previous years, even though the individual images were included in the proper climatological data products for shorter periods. This data set has been considered, and is included in the present report, with the aim of providing an historical reference for the evaluation of the SeaWiFS imagery.

The climatological annual mean (Plate 1), derived from the single-year means (Plate 2), shows the classical geographical subdivision of the Mediterranean Sea between western and eastern basins, inshore and offshore domains, northern and southern near-coastal areas. The western basin has higher *chl* values and localized mesotrophic patterns, while the eastern basin has lower *chl* values and a more uniform oligotrophic appearance. Notable features are the Alboran Sea gyre system, generated by water exchange with the Atlantic Ocean; the Ligurian-Provençal Sea enhanced patterns, due to offshore (seasonal) blooming; the Adriatic Sea coastal plumes, dominated by the impact of

river plumes; and the mesoscale gyres in the Levantine basin between the islands of Crete and Cyprus.

The climatological monthly means (Plate 3) show a seasonal cycle with higher values in the cold season – when continental runoff and vertical mixing are supposed to be the key factors contributing to the biological enrichment of surface waters – and lower values in the warm season – due to reduced runoff and stratification of the water column. The northwestern basin instead shows the sequence of winter low *chl* values (elsewhere referred to as the Gulf of Lyon "blue hole", appearing from January to March) and of large spring blooms (in April and May), sequence which has been linked to the Mistral wind seasonal pattern and the convection processes in this region, leading to deep (and bottom) water formation.

1.2 The SeaWiFS-derived *chl* Database

The SeaWiFS-derived database of the *chl* indicator, used in the present work, originates from several projects, which have built up a time series of individual daily images, collected when favourable meteorological conditions occurred over (at least part of) the European Seas. In those cases when two images were collected by SeaWiFS in the same day, due to the overlap of two consecutive orbits at high latitudes, only one value per pixel was retained in the processing chain (*i.e.* the value from the scene for which that pixel was observed with the lowest viewing angle). Each image was treated on a pixel-by-pixel basis, to correct for atmospheric contamination and to derive *chl* values. The data were originally processed using the SeaDAS software package (Fu *et al.*, 1998), with additional modifications described in Melin *et al.* (2000) and in Sturm and Zibordi (2002). Individual *chl* images, with a nominal resolution at nadir of 1.1 km, were re-mapped on an equal-area (Alber's) projection grid, covering the whole Mediterranean area, with a pixel resolution of 2 km. Composite fields, at the monthly and yearly scales, were derived from the re-mapped images, by means of simple weighted averaging techniques, while climatologies for the monthly and yearly intervals were computed using the composite images of the available period.

The SeaWiFS data were used to assess the evolution of *chl* in the Mediterranean Sea over a period of 6 years (1998-2003). The main features appearing in the SeaWiFS record are reminiscent of those already noted for the CZCS climatology. From the quantitative point of view, variations in *chl* are expected because of the differences in the sensors' characteristics and calibration (performed *a posteriori* in the CZCS case), as well as in the processing algorithms (in particular, due to the improved performance of those used for SeaWiFS, with respect to those used for CZCS, which tended to overestimate *chl* in winter, due to low sun elevation angles and consequent multiple scattering effects, in the blue band in particular, and further to overestimate *chl*

in case 2 waters, where optically active materials other than chlorophyll-like pigments contribute to water optical properties). A systematic inter-comparison of CZCS and SeaWiFS data, and of data from other sensors as well, is provided by Bricaud *et al.* (2002). In the present case, the SeaWiFS-derived *chl* values appear to be systematically lower, but consistent with the OCEAN climatological means. The main differences appear in the northwestern (and westernmost) part of the basin, where more intense blooming seems to have occurred in the SeaWiFS period.

In the present report, all SeaWiFS-derived images have been mapped to the same pixel grid and coded with the same colour bar, so that they are all directly comparable from both the geographical and the quantitative point of view. This includes Plate 9, where no colour bar could be displayed due to space limitations. The colour coding coherently represents *chl* values in mg m^{-3}. Anomalies are coded with a two-colour (blue-red) bar, also representing *chl* values in mg m^{-3}. So-called "excess anomalies" are simply coded in blue (< -1 mg m^{-3}) and green (> +1 mg m^{-3}). Numbers along the horizontal and vertical axis of the images, when present, show longitude and latitude values, respectively. Although the geographical grid includes – and the images always display – parts of the Bay of Biscay, to the north west, and part of the Black Sea, to the north east, all statistical processing showed in the reported graphics does not include the value of any pixel from these areas. Inland lakes, also displayed in the imagery, were excluded from the statistical processing as well.

Plate 1. CZCS-derived chl Climatological Annual Mean

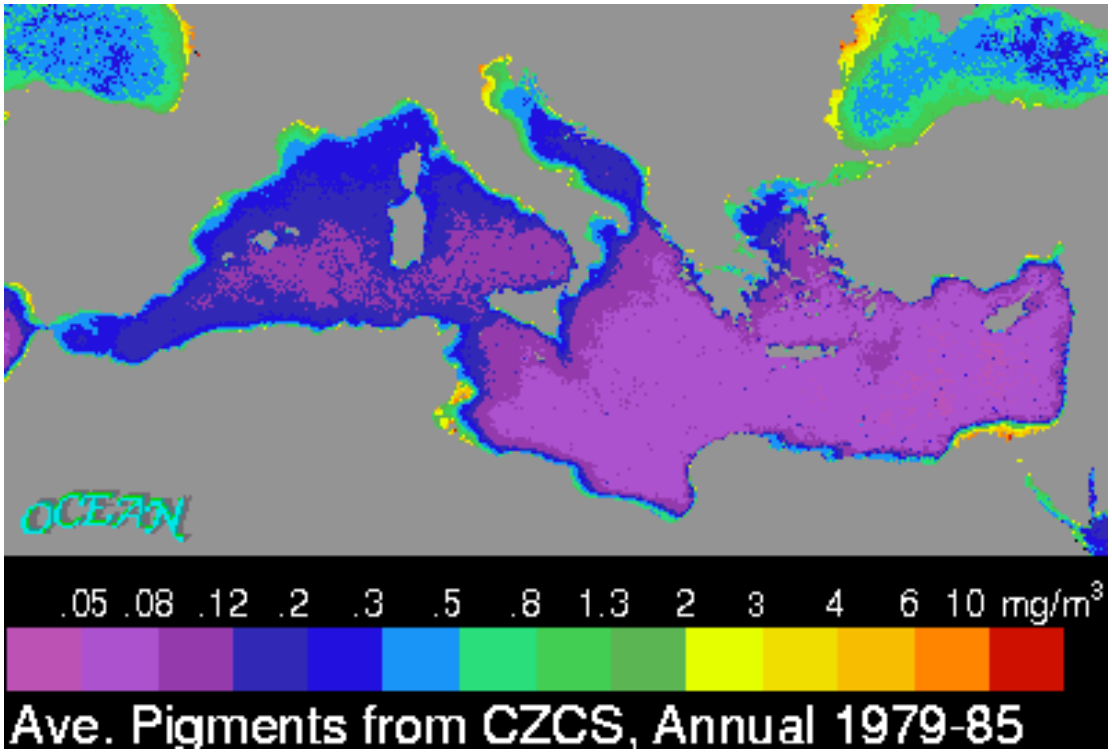

Plate 2. CZCS-derived chl Annual Means

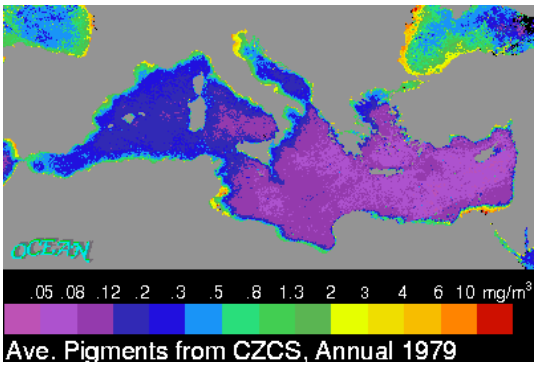

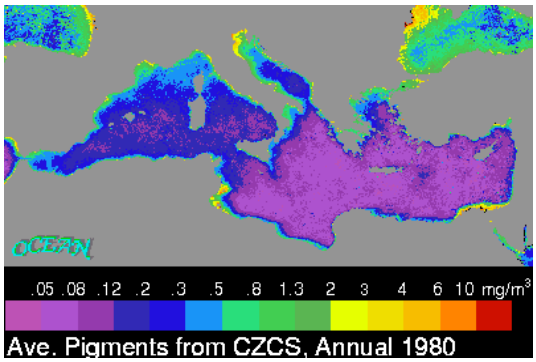

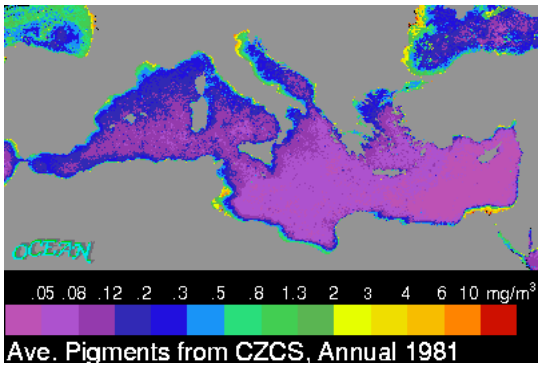

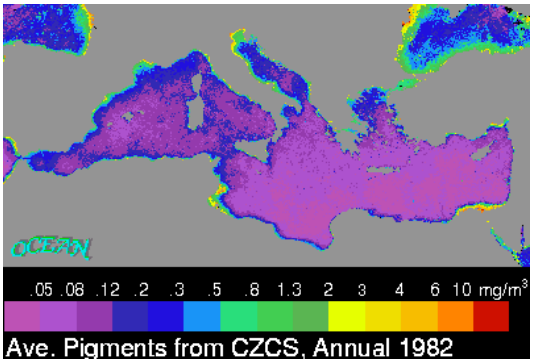

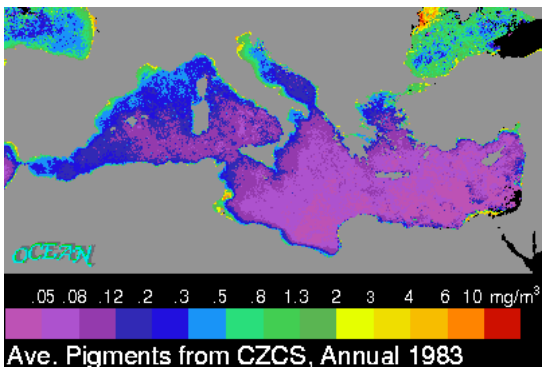

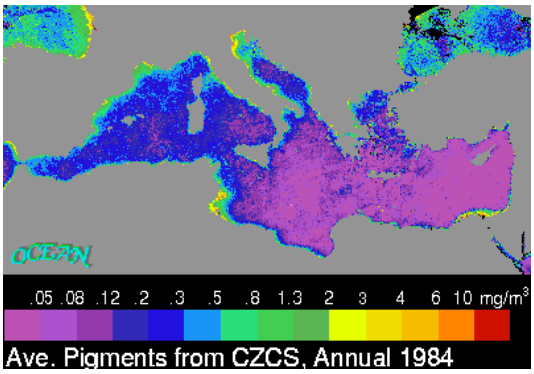

Plate 3. CZCS-derived chl Climatological Monthly Means

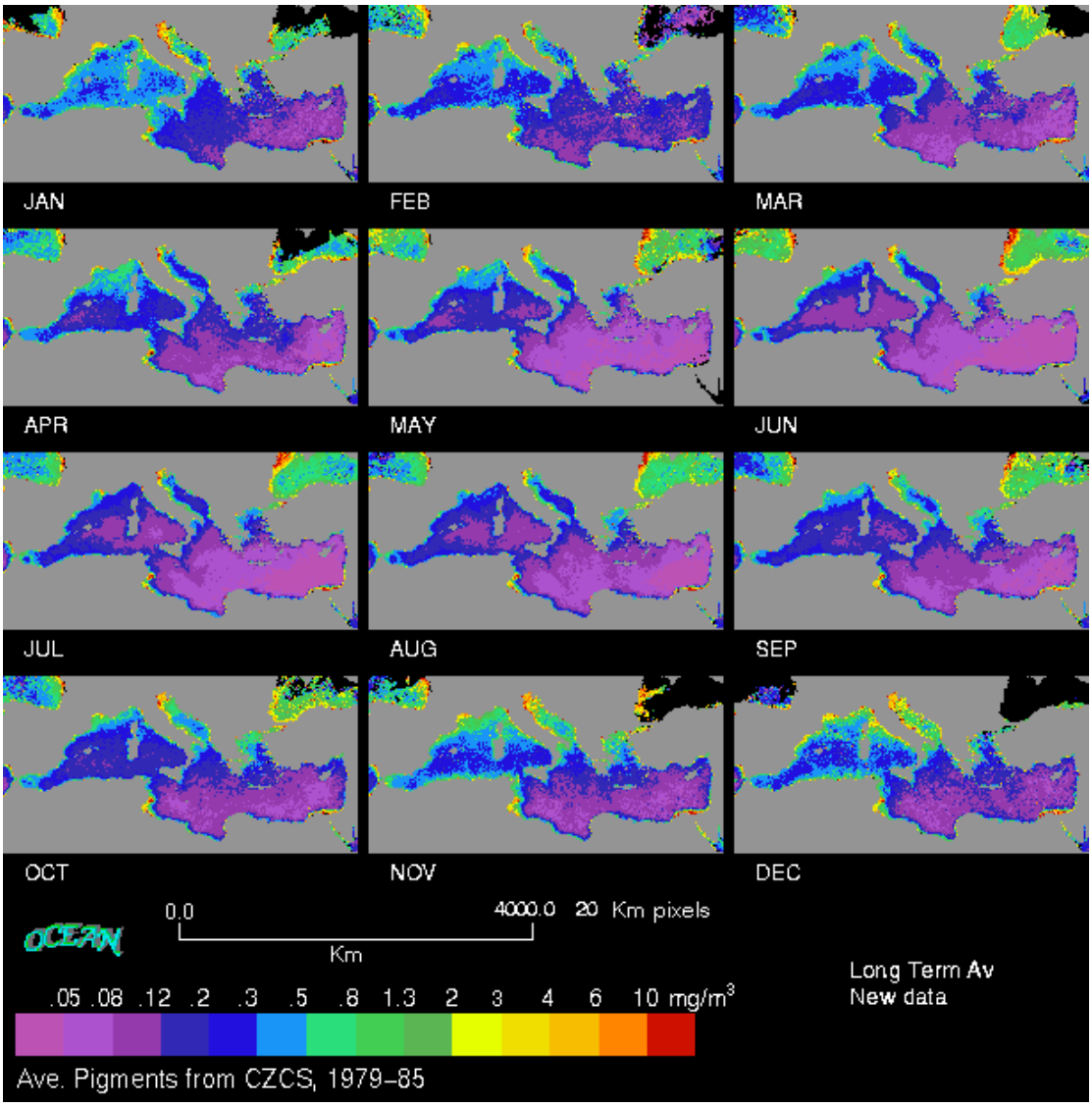

2. Interannual variability

The assessment of interannual variability in the 1998-2003 SeaWiFS-derived data set was carried out by generating annual means of *chl* and then comparing each year with the climatological data derived for the same period. The climatological annual mean (Plate 4) was computed as the average of the annual means derived for each of the 6 years available (Plate 5). Each of these, in turn, was computed both as the average of the 12 monthly means considered with equal weight, as well as the average of the monthly means weighted by the number of observations available on a pixel-by-pixel basis. A comparison by linear regression of the values obtained for each year with the two methods shows a correlation coefficient ranging from 0.9946 to 0.9965 (Plate 6), thus testifying that, in spite of the irregular coverage provided by SeaWiFS in the years considered, given the high number of realizations used to compute the averages, the mean images are only marginally affected by the specific weighting function adopted. The evaluation of interannual variability was done by computing *chl* anomalies at the annual scale, as the difference between each individual year and the climatological year. The results were mapped for each pixel both as percent as well as real values (Plate 8).

2.2 Spatial patterns in the annual means

The oligotrophic character of most sub-basins is the main feature of the Mediterranean Sea appearing in the climatological annual mean of Plate 4. The western and eastern basins are not too dissimilar, in the offshore (pelagic) domain, with an overall basin average of *chl* around 0.2 mg m^{-3}. The inshore (near-coastal) domain, on the other hand, presents higher *chl* values in the northwest and west, and lower *chl* values in the south and southeast. The high-*chl* near-coastal areas include the Ligurian–Provençal–Balearic sub-basins, and the (northern) Adriatic and Aegean Seas. This rim of enhanced pigments around most of the northern Mediterranean is associated with the impact of runoff from continental margins (*i.e.* both a direct impact due to the sediment load and one induced on the plankton flora by the associated nutrient load), but may reflect also the vertical mixing regime due to the prevailing winds, *i.e.* the Mistral over the north-western Mediterranean, the Bora over the Adriatic and the Etesians over the Aegean (Barale and Zin, 2000). Other examples of dynamical features related to mixing processes in the water column are provided by the quasi-permanent gyres due to the incoming Atlantic jet in the Alboran Sea, or by the giant filament of Capo Passero, at the southern tip of Sicily, also linked to the current system originated by the Atlantic jet flowing eastward over a steep continental slope. Where major rivers (*i.e.* the Ebro, Rhone, Po, in the western basin and the Nile, in the eastern basin) flow into the basin, coastal areas appear to be permanently under the direct influence their plumes, a feature that was already evident in the CZCS historical data set (Barale and

Larkin, 1998). Minor river discharges, or non-point sources of runoff, also have a coastal signature in the pigment field, as along the Italian coast in the Tyrrhenian Sea, along both the Italian and Albanian coastlines in the Adriatic Sea, and along the northern shores of the Aegean Sea and the Marmara Sea, where exchanges with the Black Sea also take place. In the coastal area off southern Tunisia, instead, the enhanced pigment signal is due to direct bottom reflection in an area of shallow clear waters, around the Kerkenna Island, and not to runoff patterns (Jaquet *et al.*, 1999).

The features of the climatological annual mean image appear to be recurrent in the single annual means of Plate 5. However, a certain degree of interannual variability is evident in the main spatial patterns. In particular, the size of the blooming area in the northwestern sub-basin (with *chl* ≥ 0.3 mg m^{-3}) appears to increase from 1998 to 1999, but then to decrease systematically from 2000 to 2003. Similarly, the size of the super-oligotrophic area in the southeastern sub-basin (with *chl* << 0.1 mg m^{-3}) appears to increase systematically in the second half of the period covered by SeaWiFS. This is reflected in the variability of the average basin value of *chl* derived from the annual means (*i.e.* a single *chl* value computed as the total average of all pixels composing each annual image) shown in Plate 7. The trend appearing in this variability indicates a general decrease in the *chl* indicator, over the period of SeaWiFS coverage, estimated to be about 10% of the climatological average value for the entire basin.

2.2 Blooming Anomalies in the Annual Means

The SeaWiFS-derived *chl* annual anomalies shown in Plate 8 highlight the geographical spread and intensity of blooming patterns, which differed in each year from the climatological annual mean. The basin shows mostly positive anomalies in the first 3 years and mostly negative anomalies in the second 3 years. The northwestern sub-basin displays a *quasi*-systematic counter-trend, with respect to the remainder of the western basin, both in a negative sense, as in 1998-1999, as well as in a positive sense, as in 2002. The northeastern sub-basin also seems to show a recurring counter-trend, with respect to the eastern basin, again both in a negative sense, as in 1998-1999, as well as in a positive sense, as in 2003. Inshore areas can also present sharp fluctuations (absolute value ≥ 0.1 mg m^{-3}) from negative to positive anomalies, and *vice versa*, as apparent along the Catalan coast or in the northern Adriatic sea (see *e.g.* 1998 *vs* 2003, in both cases). Very high anomalies (absolute value ≥ 10 mg m^{-3}), labeled in Plate 8 as "excess anomalies", are seen to recur only along the shoreline, in shallow waters (near the Island of Jerba) or around river plumes (south of the Po river delta).

Plate 4. SeaWiFS-derived chl Climatological Annual Mean

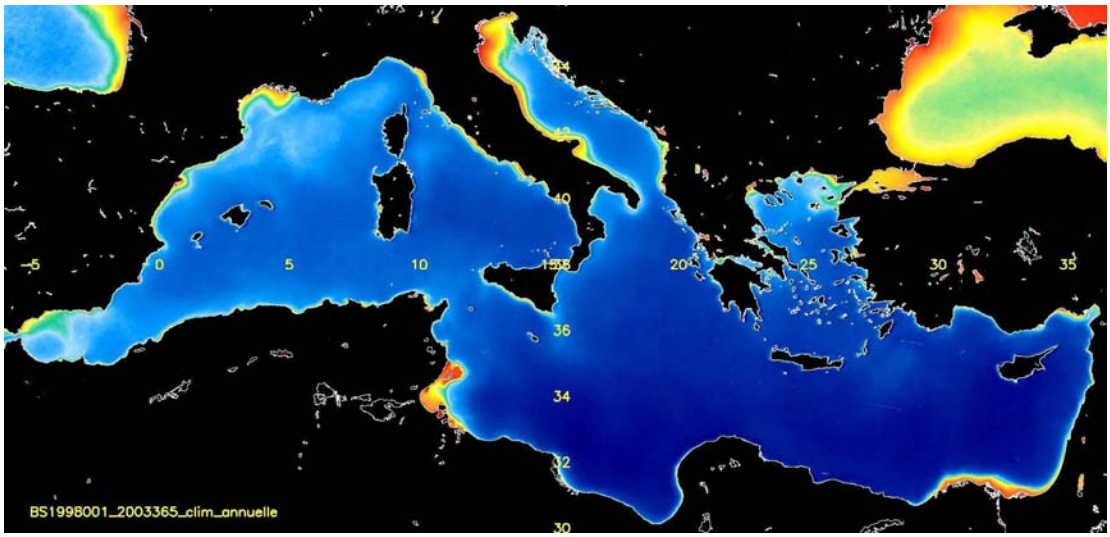

climatological annual mean

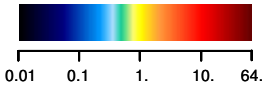

chl [mg m^{-3}]

Plate 5. SeaWiFS-derived chl Annual Means

annual mean 1998

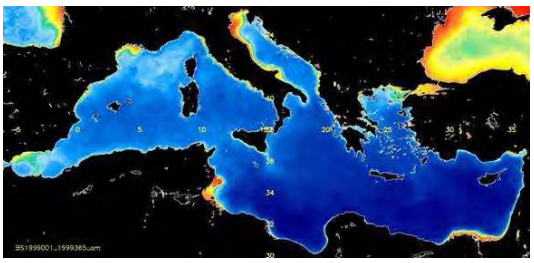

annual mean 1999

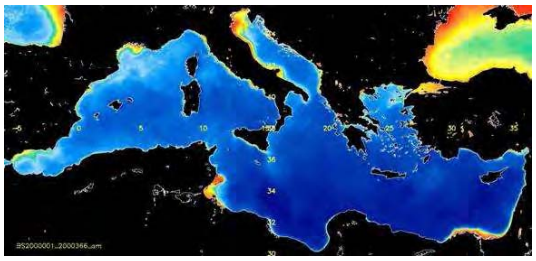

annual mean 2000

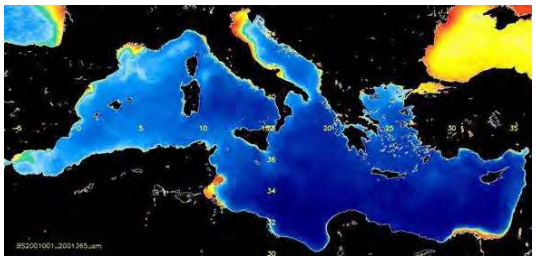

annual mean 2001

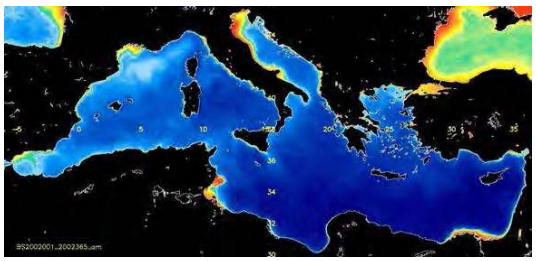

annual mean 2002

annual mean 2003

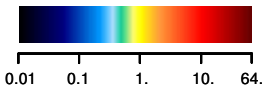

chl [mg m^{-3}]

Plate 6. Annual Mean chl vs Annual Weighted Mean chl

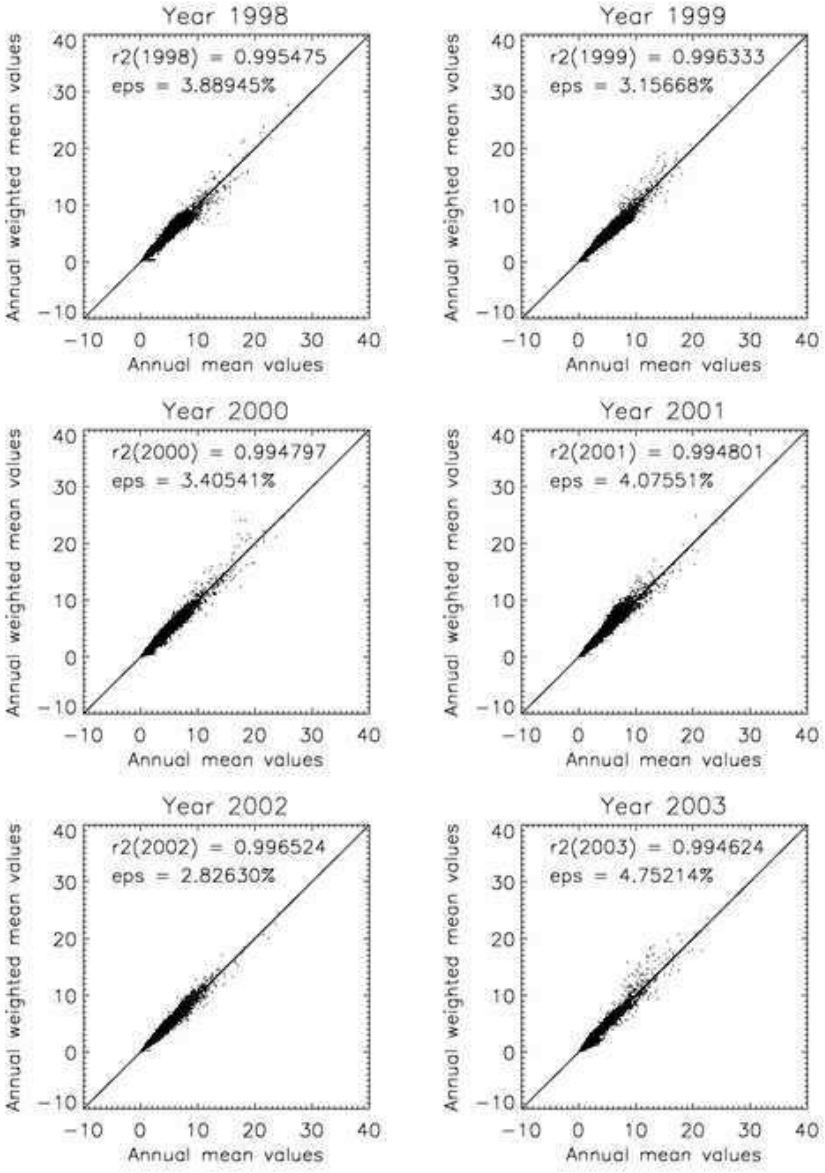

Plate 7. Trend of the chl Annual Means (average basin value)

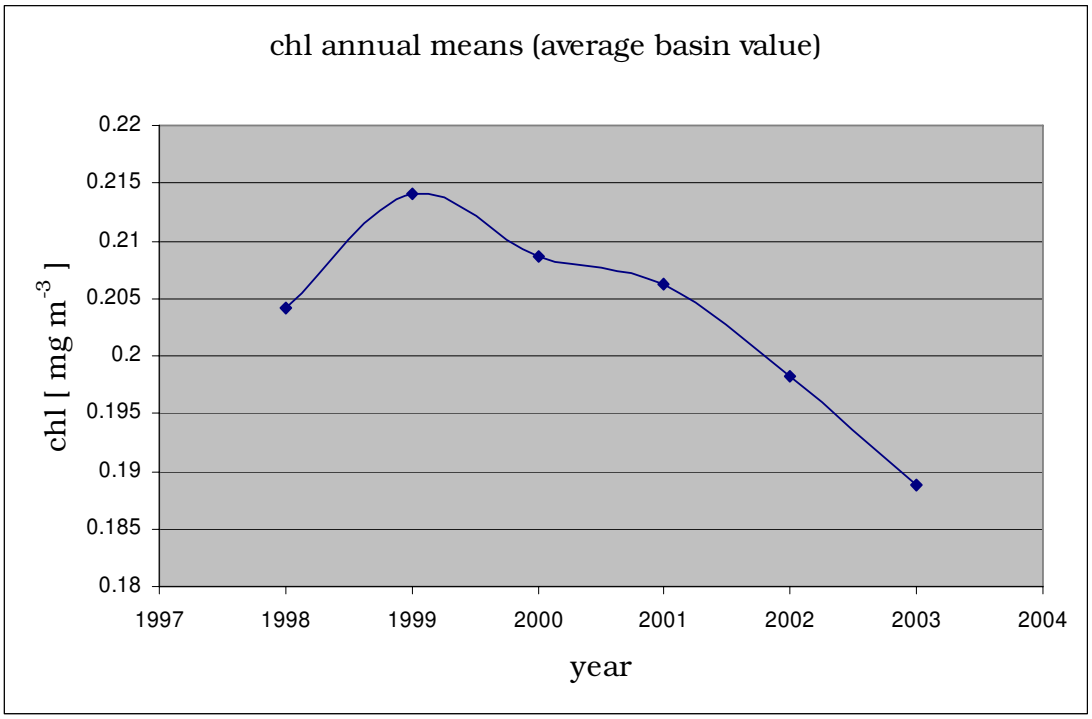

Plate 8. SeaWiFS-derived chl Annual Anomalies

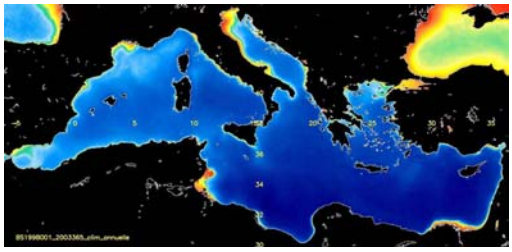

climatological annual mean

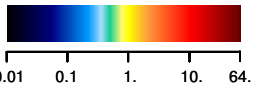

chl [mg m^{-3}]

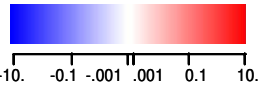

anomalies [mg m^{-3}]

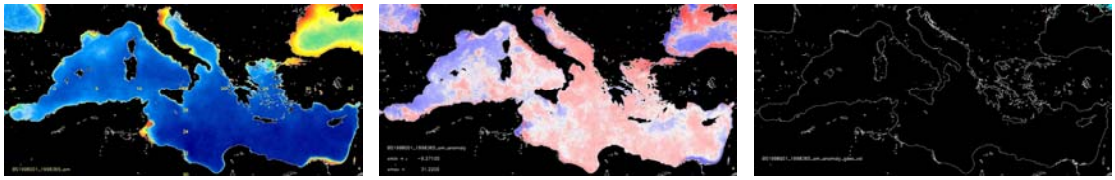

1998

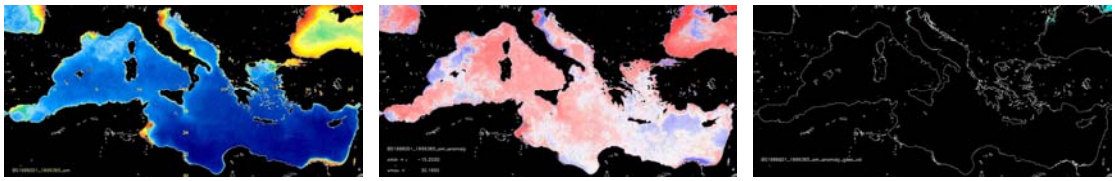

1999

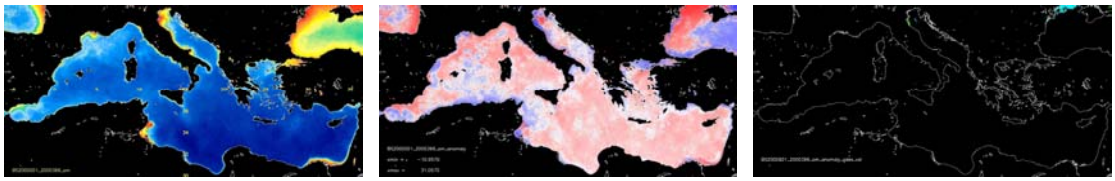

2000

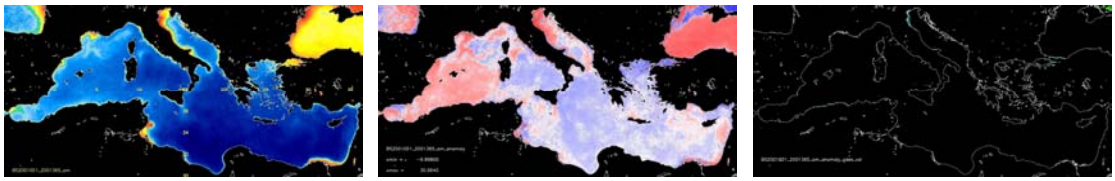

2001

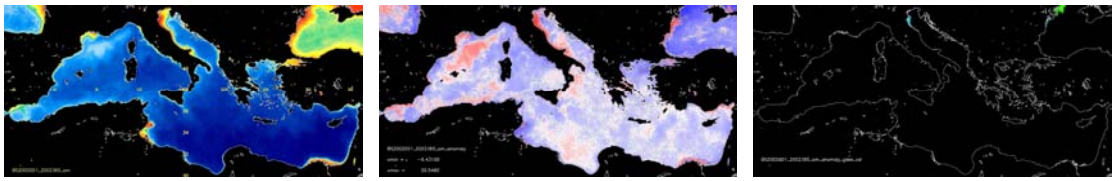

2002

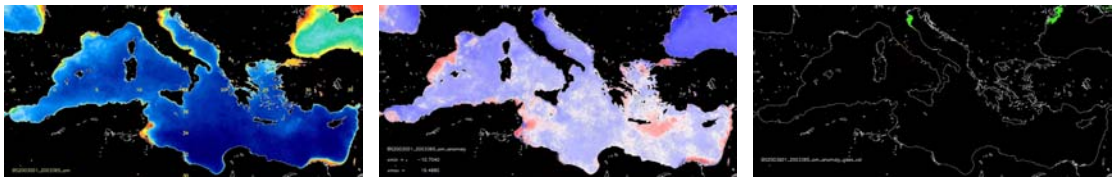

2003

Left panels: annual mean concentration of chl [mg m^{-3}]
Middle panels: chl anomalies [mg m^{-3}] as mean concentration – climatological value
Right panels: excess anomalies (blue < -1 mg m^{-3}, green > +1 mg m^{-3})

3. Seasonal variability

The assessment of seasonal variability in the 1998-2003 SeaWiFS-derived data set was carried out by generating climatological monthly means of *chl* (*i.e.* 12 monthly means generated as the average of the 6 realizations available for each month in the period 1998-2003; see Plate 9), and then comparing single monthly means with the climatological record. Thus, a time component was coupled to the evaluation of space patterns, by computing the sequence of *chl* anomalies at the monthly scale, as the difference between each individual month and the corresponding climatological month. Again, the results were mapped for each pixel, both as percent as well as real values (Plates 13 to 24). As in the annual case, "excess" anomalies (absolute value ≥ 10 mg m^{-3}), generally recurring for pixels in near-coastal areas, were also mapped separately, in order to retain a first order assessment of potential hot spots, both in space and time, for anomalous blooming.

3.1 Spatial Patterns and Trends in the Monthly Means

The spatial patterns appearing in the climatological monthly means of Plate 9 are not dissimilar from those observed at the annual scale, but show enhancements over (variable) seasonal periods. The whole Mediterranean Sea presents higher *chl* values in January, February and March (period referred to as winter, in the following), with peak blooming occurring earlier (February) in a few sub-basins and systems (*e.g.* the Alboran Sea and the Algerian Current, in the western basin) or later on (March) in others (*e.g.* the Ligurian-Provençal Sea, in the western basin, but also the northeastern Levantine basin, in the area of the Rhodes Gyre). While blooming continues in some areas (*i.e.* the northwest, but also the Alboran Sea) in April, May and June (spring, in the following), signs of oligotrophic conditions appear in the eastern basin as early as March (but as late as June in the west, *i.e.* in the Tyrrhenian Sea). The oligotrophic state prevails in July, August and September (summer), everywhere in the eastern basin, except for coastal plumes, and in the interior of the western basin. Elsewhere in the western basin, the northern near-coastal area of the Ligurian-Provençal Sea seems to retain higher *chl* values, even in summer, similarly to the southern near-coastal area impacted by the incoming (permanent) Atlantic jet. These conditions appear to relax in October, November and December (fall), as early as October in the western basin, starting from the southwest, but only in December in the eastern one, when blooming seems to take up again, in preparation for the winter peak.

In the preceding analysis, the SeaWiFS-derived time series presents a seasonal cycle analogous to the one appearing in the historical CZCS data set, *i.e.* a bimodal pattern with *maxima* in the colder season, from late fall to early spring, followed by *minima* in the warmer one, from

late spring to early fall. This is substantiated by the fluctuation of the average basin value of *chl* derived from the monthly means (*i.e.* a single *chl* value computed as the total average of all pixels composing each monthly image), shown in Plate 10. As noted already for the annual means, the *chl* indicator displays also a decreasing trend, over the period of SeaWiFS coverage, estimated in this case, by linear regression, to be about 20% of the climatological average value for the entire basin.

The climatological seasonal trend (Plate 11), obtained computing an average basin value of the *chl* indicator from the climatological monthly mean images, suggests that, from a bio-geo-chemical point of view, the Mediterranean Sea as a whole presents a behaviour similar to that of a sub-tropical basin, where the light level is never a limiting factor, so that its decrease in winter does not inhibit algal growth, but the nutrient level always is (Barale, 2000). In such a scenario, higher *chl* values would occur in the cold, windy and wet (winter) season, and would be related to the biological enrichment of surface waters due to surface cooling, vertical mixing and continental runoff – as opposed to lower *chl* values occurring in the warm, calm and dry (summer) season, when the water column is strongly stratified and no nutrient supply, from coastal zones or deeper layers, is readily available.

Unlike what is seen in the historical CZCS data set, though, absolute *maxima* do not appear in January and later in (November and) December. Indeed, peak *chl* values now occur in February and March, with reduced values in January and even more so in December. Hence, the climatological seasonal cycle in the SeaWiFS-derived time series shows that, after the summer low, *chl* grows systematically in fall, only to reach its absolute *maximum* in the middle of winter and then decrease rapidly in spring, toward its summer *minimum* again. This does not affect the general validity of the sub-tropical scenario, described earlier when considering the cycle of the entire Mediterranean basin, but points to the fact that some regions, namely the western sub-basins, have a somewhat different seasonality. The difference is so pronounced, in fact, that it affects basin statistics, when integrated *chl* values are considered to summarize the behaviour of the basin as a whole.

The interannual variability of this seasonal cycle is illustrated in Plate 12, where average basin values of the *chl* indicator from corresponding monthly means are plotted against time – subdivided in winter and spring plots, in Plate 12(a), as well as summer and fall plots, in Plate 12(b). The winter plot shows that the highest average basin value of *chl* can (almost) be reached already in January, and then maintained for the following months (as in 1998, 2000 and 2002), but it can also be delayed to February (as in 2001) or even to March (as in 1999 and 2003). In spring, the *chl* values drop rapidly and systematically from winter to summer levels, in all years considered. The summer plot

shows that the lowest average basin value of *chl* is reached (almost) always in August (the only exceptions occurring in 2000 and even more so in 2001, when actually the *chl* value increased in August), but that it varies very little throughout the entire season. In fall, the *chl* values rise, again rather systematically, from summer to winter levels. Seasonal excursion of the *chl* average basin values, in a given year, can be on the order of 10-20% in winter; as high as 20-40% in spring, the largest observed; only 10% in summer; and then 20-30% in fall.

While the Mediterranean basin as a whole seems to follow such a model, significant departures occur in some areas, and in particular in the northern sub-basins. Notably, the Adriatic Sea and the Aegean Sea display a late winter and, mostly, early spring (April) enhancement in *chl* values, superimposed to the general annual trend. Local conditions describing a combination of seasonal signatures can be recognized also elsewhere, in both the western basin – where the Alboran Sea *e.g.* presents the additional feature of coastal *chl* enhancement in early spring – and in the eastern basin – where the Rhodes Gyre core, after reaching a late winter (March) *chl maximum*, maintains its characteristics throughout the year, even appearing in summer months as the only, isolated, offshore spot of high *chl* in the super-oligotrophic basin.

The Ligurian-Provençal Sea deserves a special reference, in this list of exceptions, for displaying, primarily in the Gulf of Lyon, a rather different, almost opposite, seasonal cycle. In fact, the lowest *chl* values appear in winter, and are followed by a massive bloom in March and April. This feature, the most pronounced of the entire Mediterranean Sea, continues to be identifiable even throughout summer and fall. In this area, the lower *chl* values of the winter season are originated when strong northerly Mistral winds blow from the continental landmass onto the sea, so that the resulting deep convection processes, triggered systematically by this particular wind regime, can mix surface waters down to 1500-2000 m of depth (THETIS Group, 1994). This seems to be particularly true for the Lyons Gyre, an area of deep-water formation – *i.e.* the so-called "blue hole" already seen in the historical CZCS data set – where the lack of high *chl* in winter is linked to the extreme conditions generated by the overturning of the entire water column. This seasonality would be closer to that of a sub-polar basin, rather than a sub-tropical one, with lower pigment concentration in winter, because of reduced light or actually, more important in this case, because of the deep vertical mixing and turbulence due to the prevailing wind field, which prevents algae to be stabilized in the upper well-lit layers. The ensuing spring bloom, then, would be triggered by the relaxation of these conditions, when the wind field reduces its impact, the water column – enriched in nutrient content by the prolonged period of deep convection – becomes sufficiently stable, and stratification occurs in the basin.

It must be noted, however, that the period of deep convection appeared to be longer in the CZCS climatological sequence, since the monthly mean images showed a larger "blue hole", extending also in the Ligurian Current region, from late fall to early spring. The feature, occurring earlier in December, and then most intensely in January, February and March as well, now can hardly be recognized in December, starts to become evident in January, and is obvious only in February, while extensive blooming takes place already in March. Interestingly enough, no "blue hole" was manifest in the imagery of fall of 1997 (not shown here), when the SeaWiFS time series got started. This apparent lack of deep convection in the Gulf of Lyon, was followed by the least pronounced and shortest spring bloom observed in the same area for the 6 years considered. This testifies once more the importance of wind-induced processes in the biological cycles of the northwestern Mediterranean Sea, where the enrichment of surface waters supports a large biomass of primary and secondary producers, as well as a highly developed food web including a sizeable standing population of fin whales, *Balaenoptera physalus* (see Barale *et al.*, 2002, and references therein).

3.2 Blooming Anomalies in the Monthly Means

The SeaWiFS-derived *chl* monthly anomalies shown in Plates 13-24 highlight the geographical spread and intensity of blooming patterns, which differed in each month from the corresponding climatological monthly mean. The time series shows that anomalies can occur just about anywhere in the basin, even though they are most noticeable in the areas of intense blooming, and in all periods of the year. There are at least three general types of anomalies, which seem to be of particular interest. The first is a basin-wide anomaly, when the greater part of the Mediterranean Sea appears to be above or below the climatological mean value (*e.g.* December 1998, positive; December 2002 or 2003, negative). The second kind of anomaly shows the western and the eastern basins oscillating in opposite ways (*e.g.* September 2000, western basin mainly negative, eastern mainly positive; and February 2001, opposite situation). In general, though, the most common anomalies are of a third kind, which involves only a specific sub-basin or near-coastal area. In the western basin, the Ligurian-Provençal Sea and the Alboran Gyres – Algerian Current system, where the most intense blooming occurs, are once again the sites of recurring anomalies. As an example, both positive and negative anomalies can be seen, in sequence, between February and March 1998 in these areas. In the eastern basin, the gyre system south and east of the Island of Crete, and the Rhodes Gyre in particular, displays similar characteristics (*e.g.* negative anomalies in March 1998, and positive in April 2003). Even though a general trend does not seem to be easily identifiable, it appears that short-term anomalies like those in the monthly record can provide important information about regional conditions linked to local blooming events.

Plate 9. SeaWiFS-derived chl Climatological Monthly Means

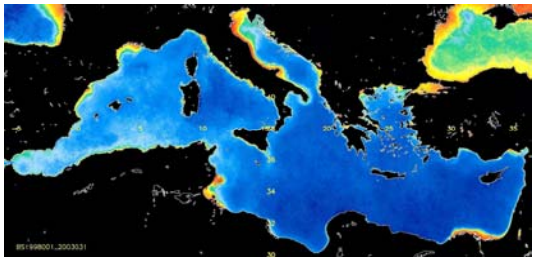

January

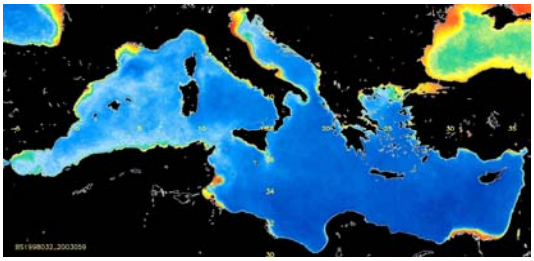

February

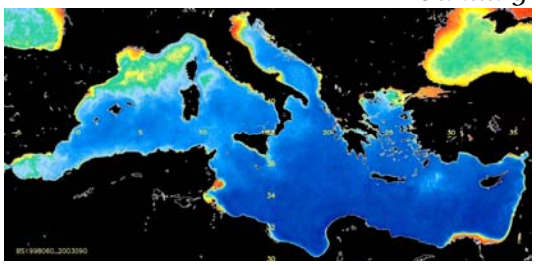

March

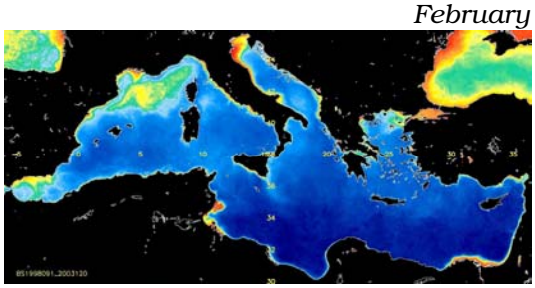

April

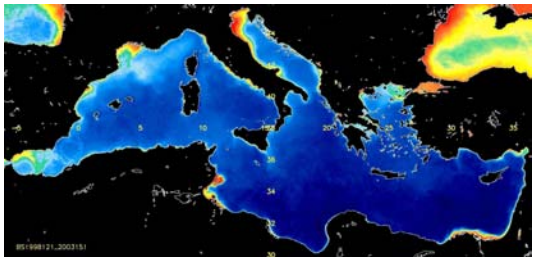

May

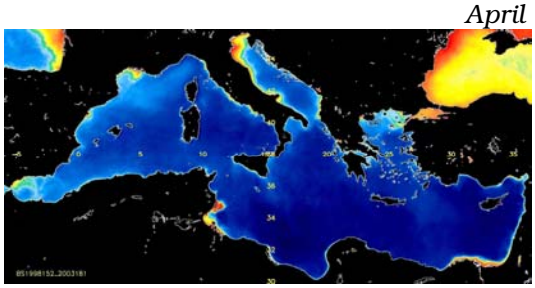

June

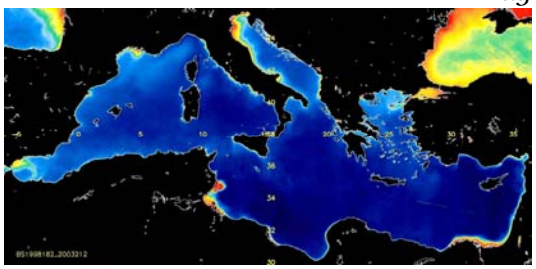

July

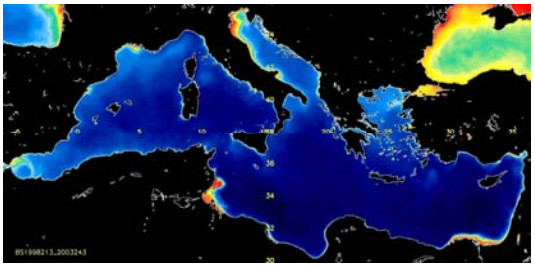

August

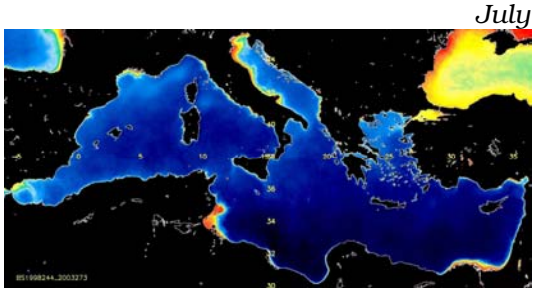

September

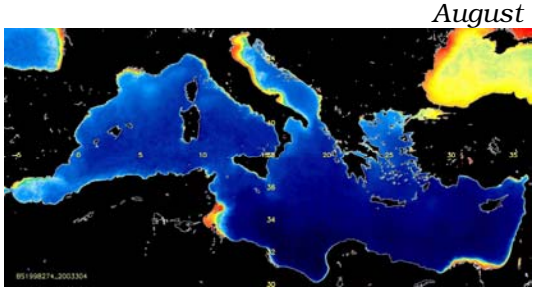

October

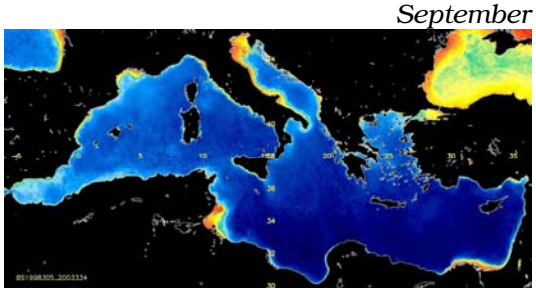

November

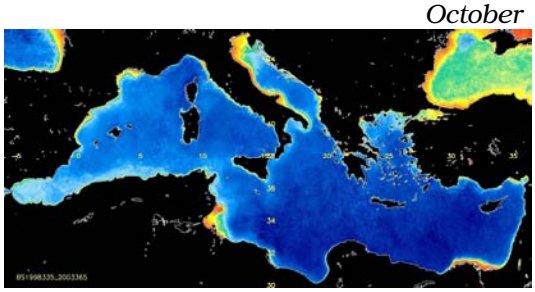

December

Plate 10. Trend of chl Monthly Means (average basin value)

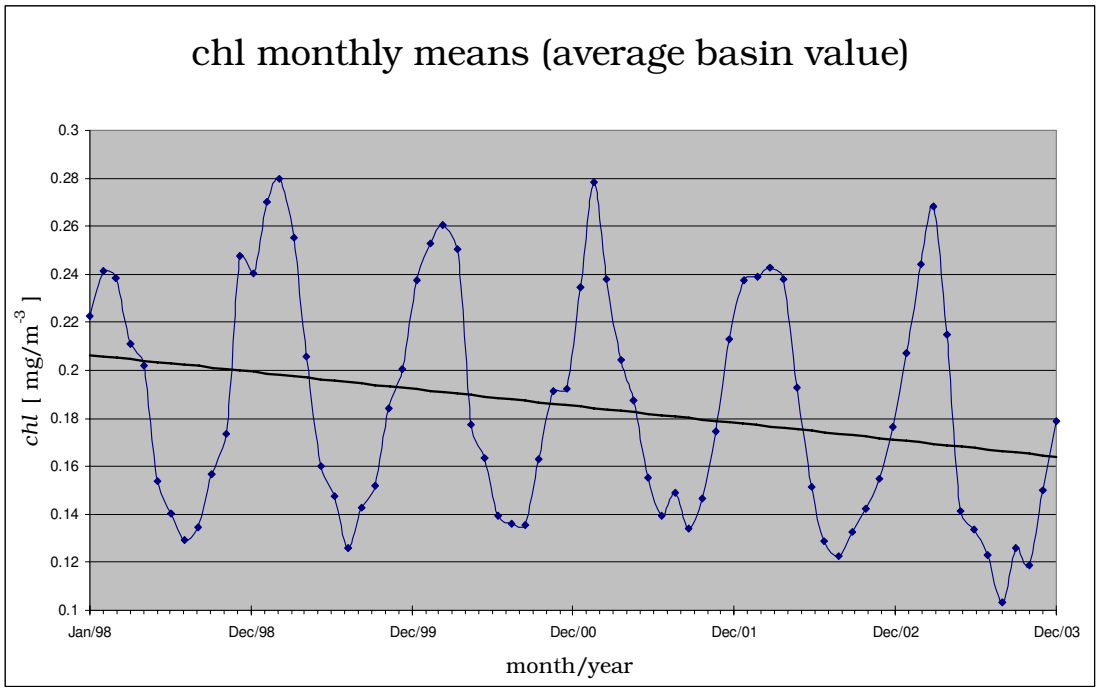

Plate 11. Climatological Monthly Means (average basin value)

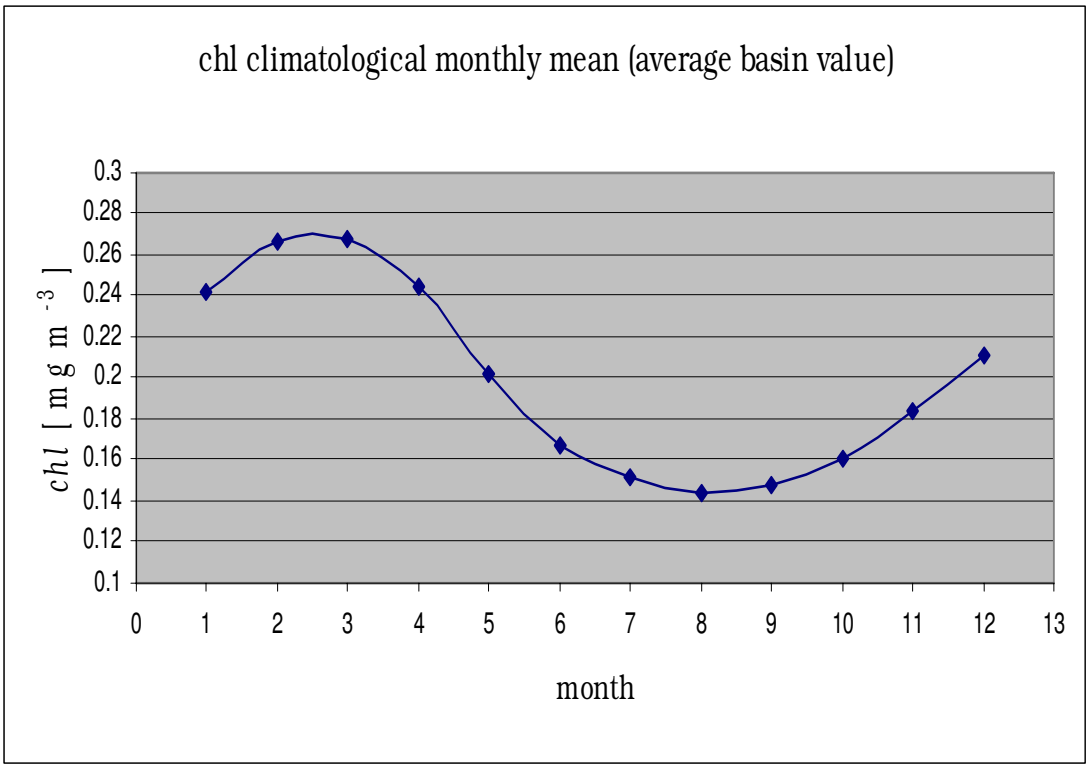

Plate 12 (a). Winter & Spring Variability of chl Monthly Means

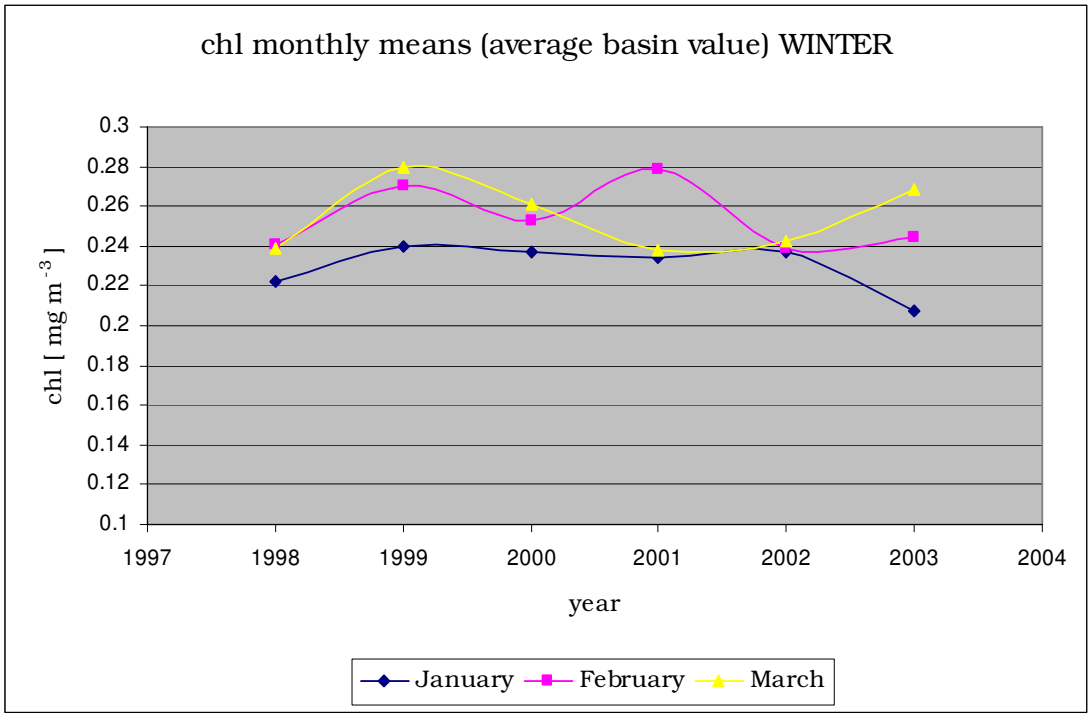

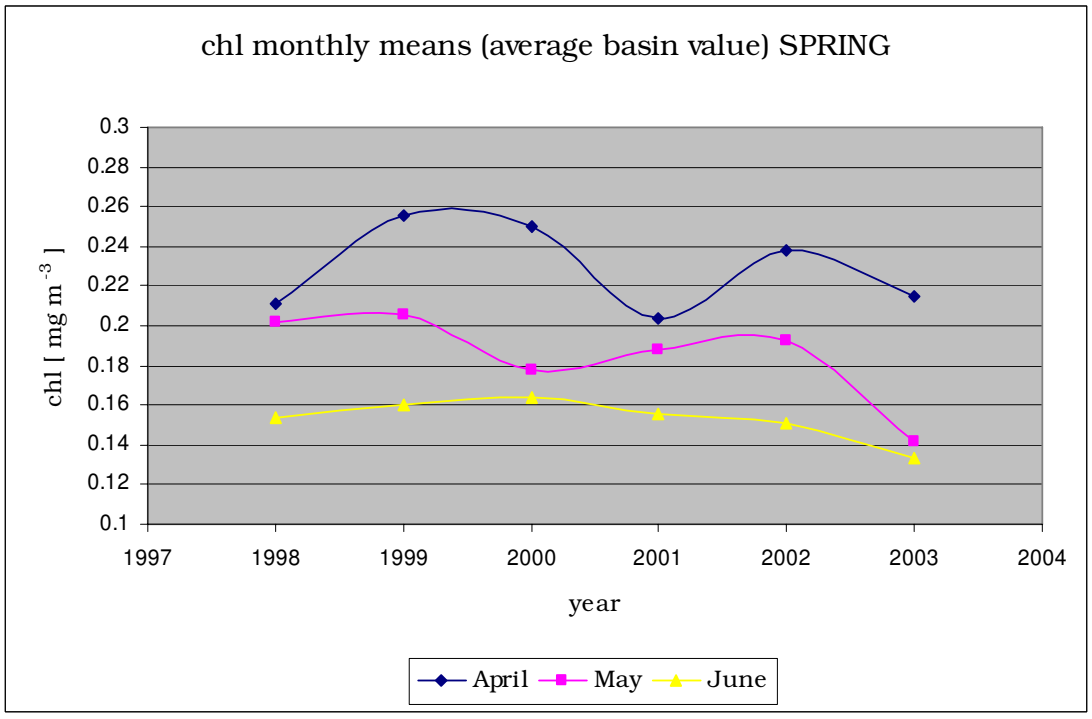

Plate 12 (b). Summer & Fall Variability of chl Monthly Means

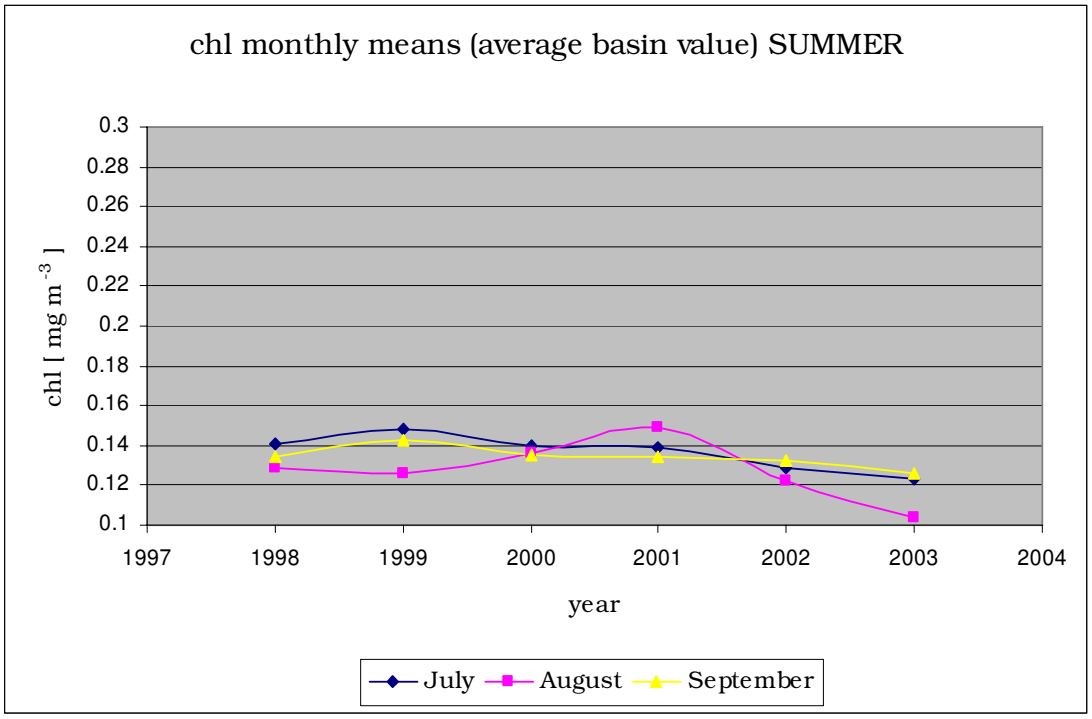

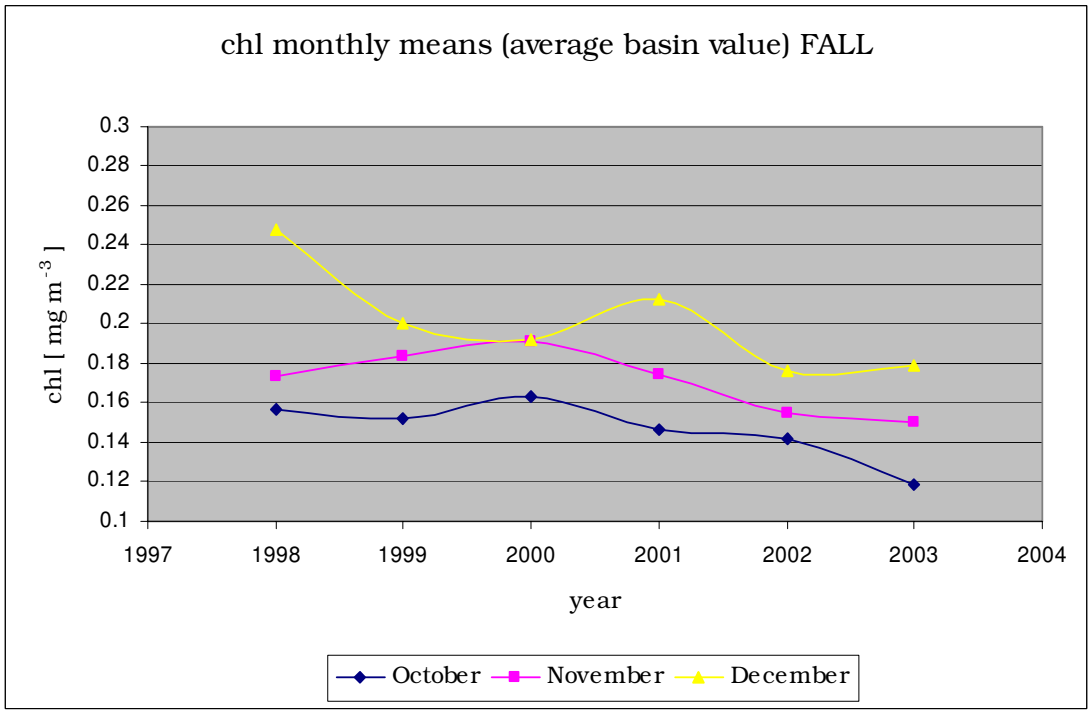

Figure 13. Monthly Anomalies: January

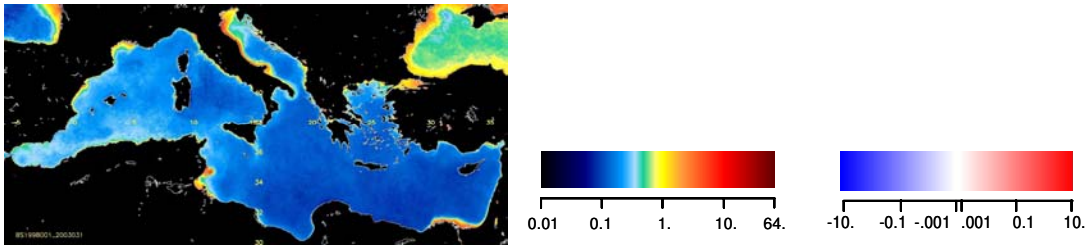

climatological monthly mean *chl [mg m^{-3}]* *anomalies [mg m^{-3}]*

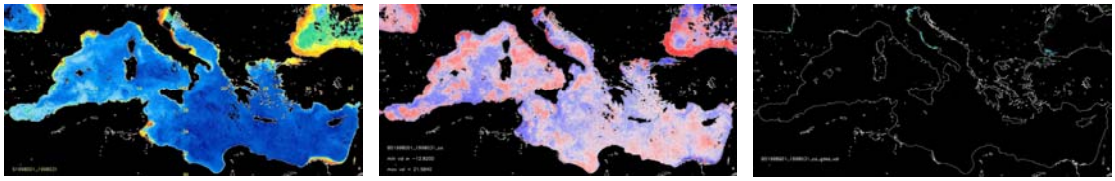

Jan 1998

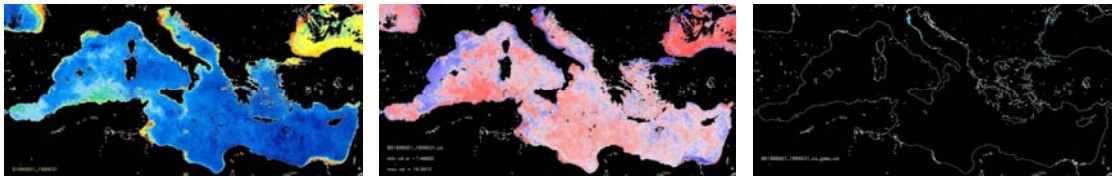

Jan 1999

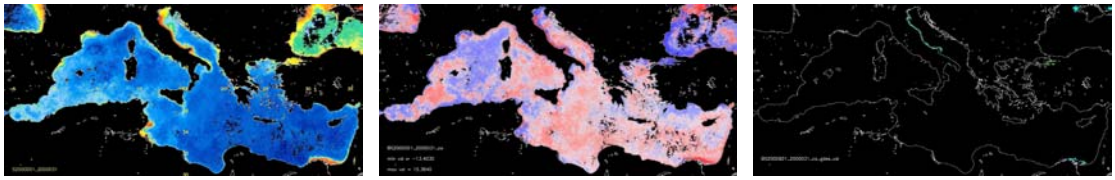

Jan 2000

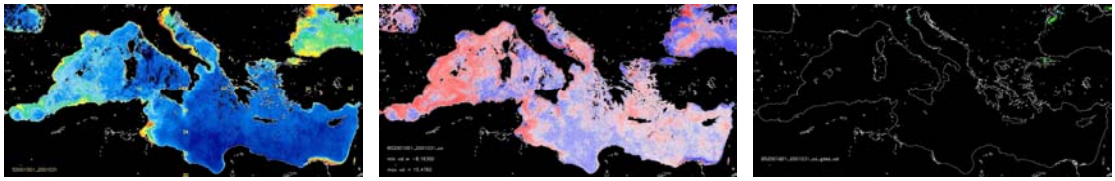

Jan 2001

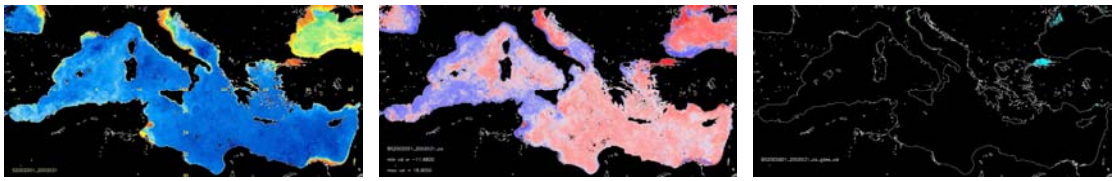

Jan 2002

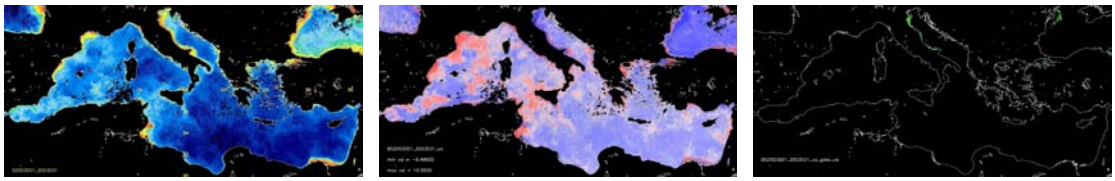

Jan 2003

Left panels: monthly mean concentration of chl [mg m^{-3}]
Middle panels: chl anomalies [mg m^{-3}] as mean concentration – climatological value
Right panels: excess anomalies (blue < -1 mg m^{-3}, green > +1 mg m^{-3})

Figure 14. Monthly Anomalies: February

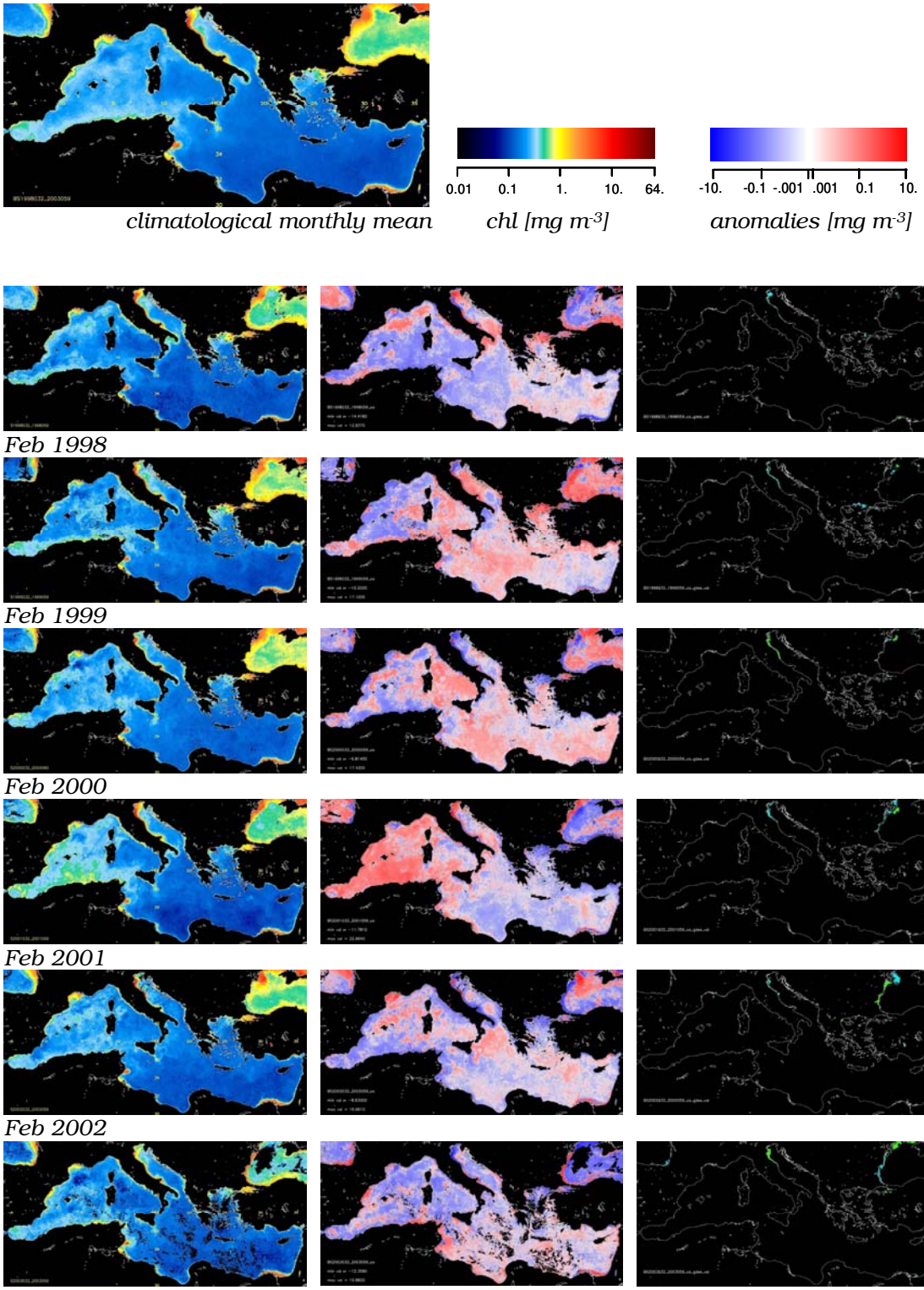

Left panels: monthly mean concentration of chl [mg m^{-3}]
Middle panels: chl anomalies [mg m^{-3}] as mean concentration – climatological value
Right panels: excess anomalies (blue < -1 mg m^{-3}, green > +1 mg m^{-3})

Figure 15. Monthly Anomalies: March

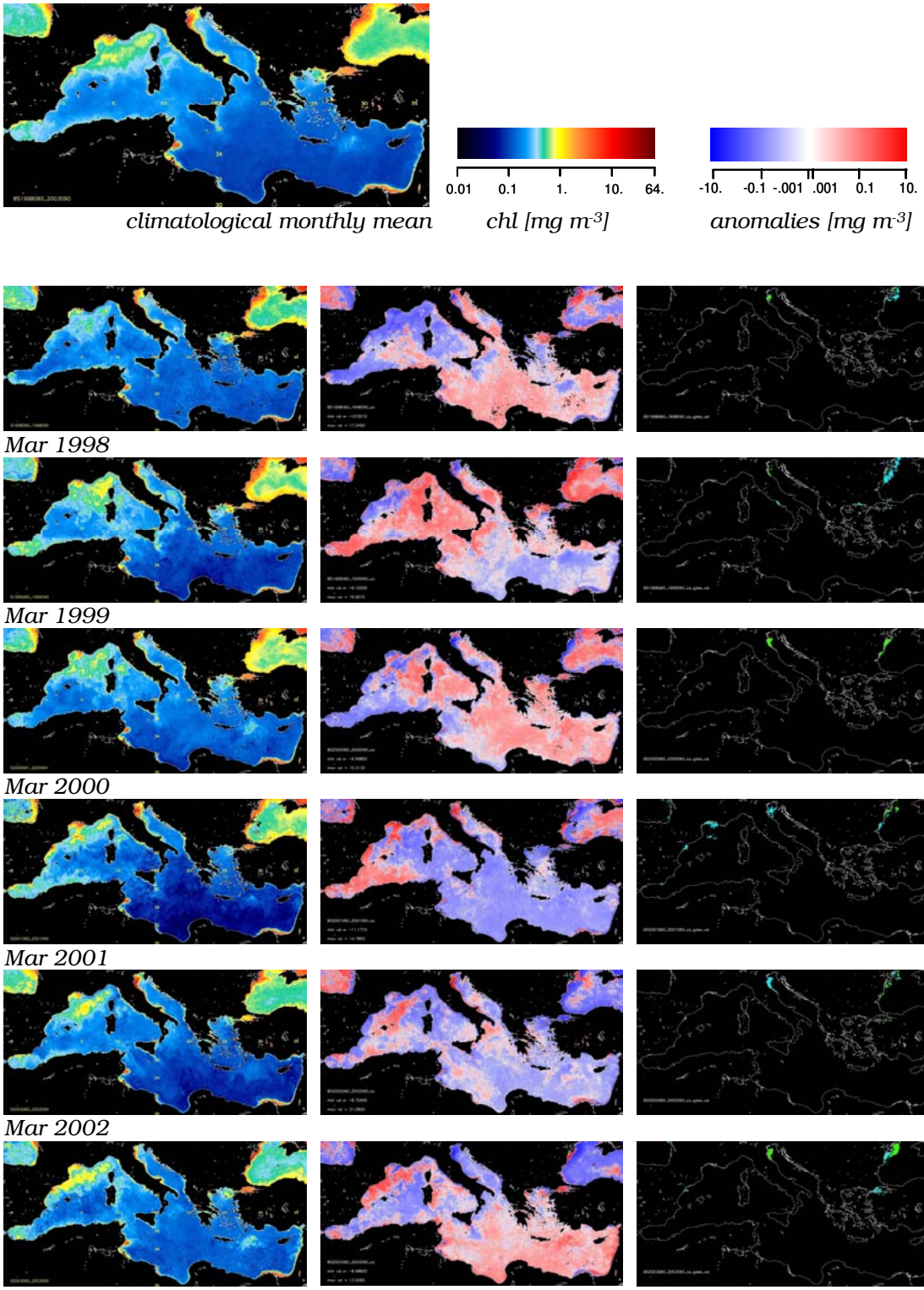

Left panels: monthly mean concentration of chl [mg m^{-3}]
Middle panels: chl anomalies [mg m^{-3}] as mean concentration – climatological value
Right panels: excess anomalies (blue < -1 mg m^{-3}, green > +1 mg m^{-3})

Figure 16. Monthly Anomalies: April

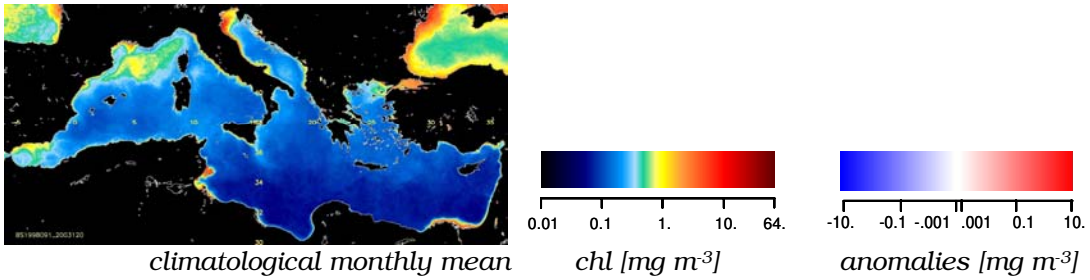

climatological monthly mean *chl [mg m^{-3}]* *anomalies [mg m^{-3}]*

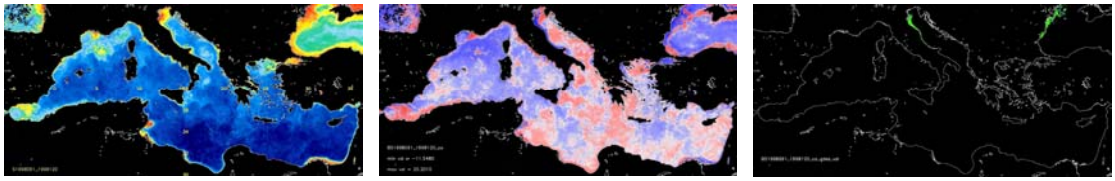

Apr 1998

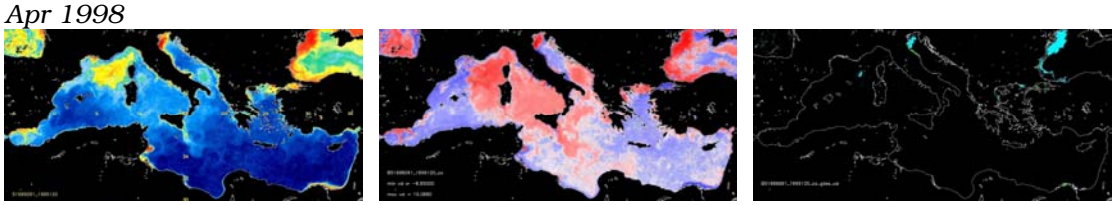

Apr 1999

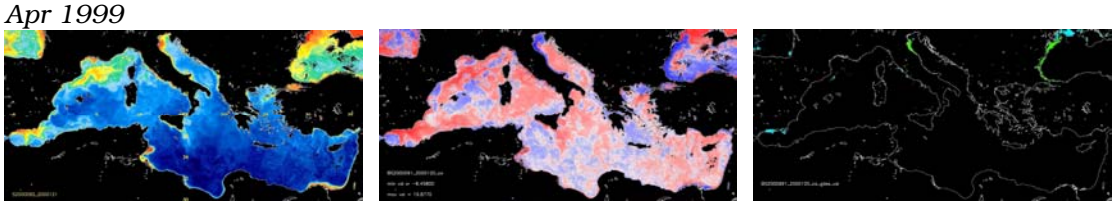

Apr 2000

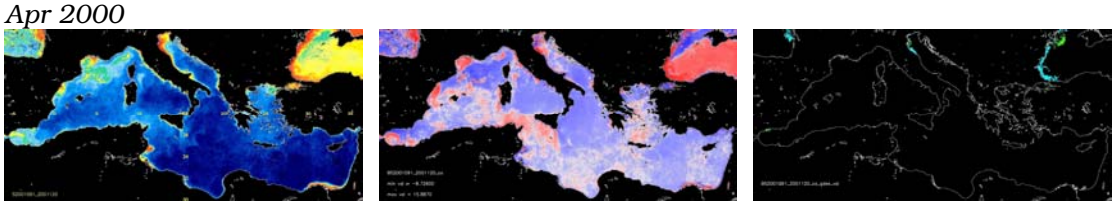

Apr 2001

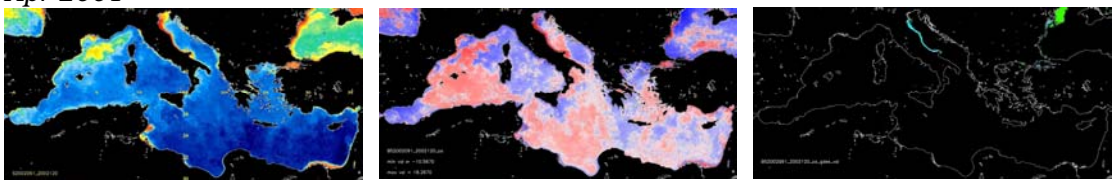

Apr 2002

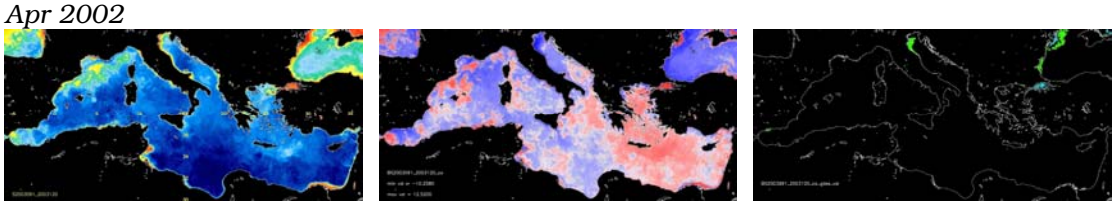

Apr 2003

Left panels: monthly mean concentration of chl [mg m^{-3}]
Middle panels: chl anomalies [mg m^{-3}] as mean concentration – climatological value
Right panels: excess anomalies (blue < -1 mg m^{-3}, green > +1 mg m^{-3})

Figure 17. Monthly Anomalies: May

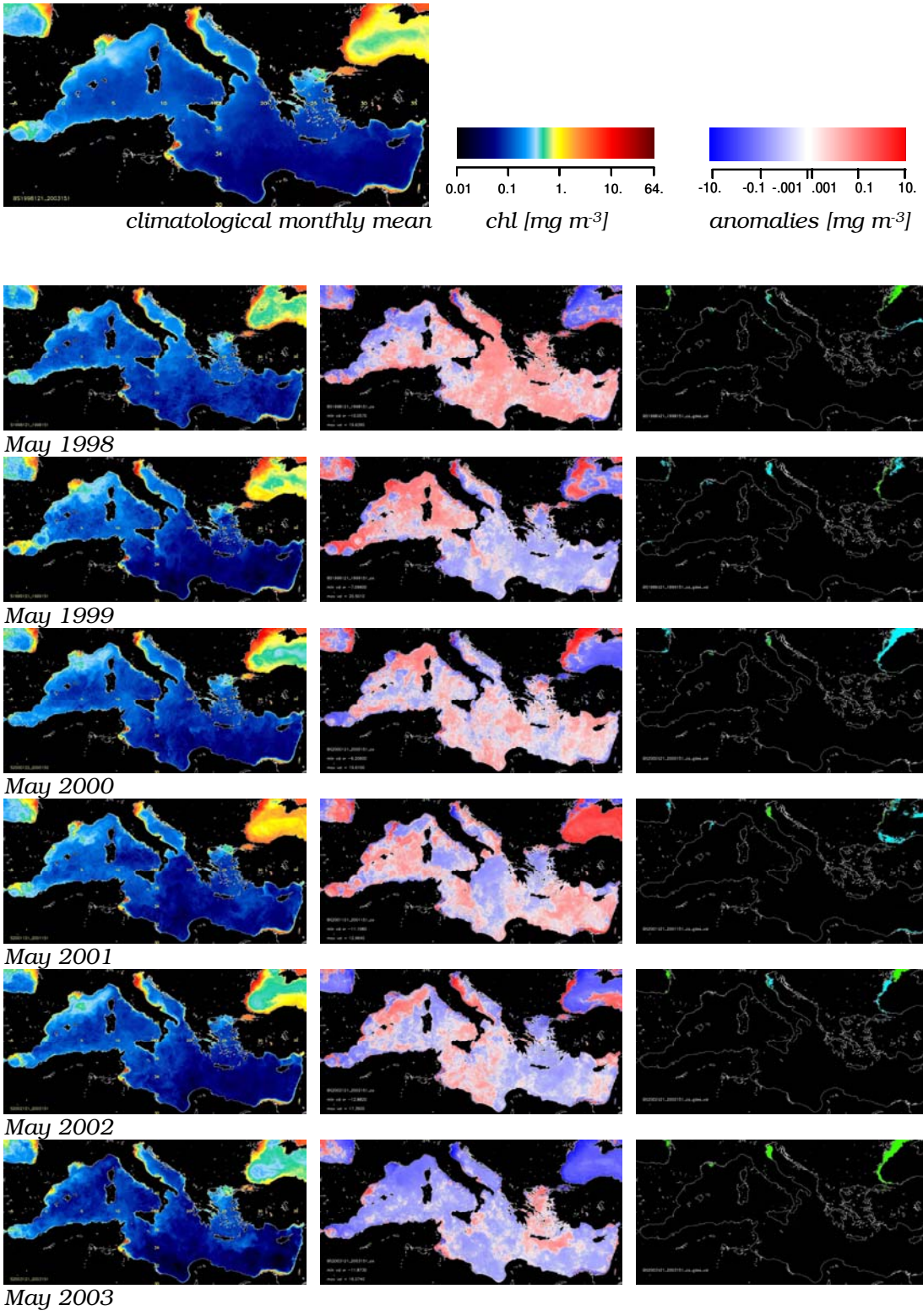

Left panels: monthly mean concentration of chl [mg m^{-3}]
Middle panels: chl anomalies [mg m^{-3}] as mean concentration – climatological value
Right panels: excess anomalies (blue < -1 mg m^{-3}, green > +1 mg m^{-3})

Figure 18. Monthly Anomalies: June

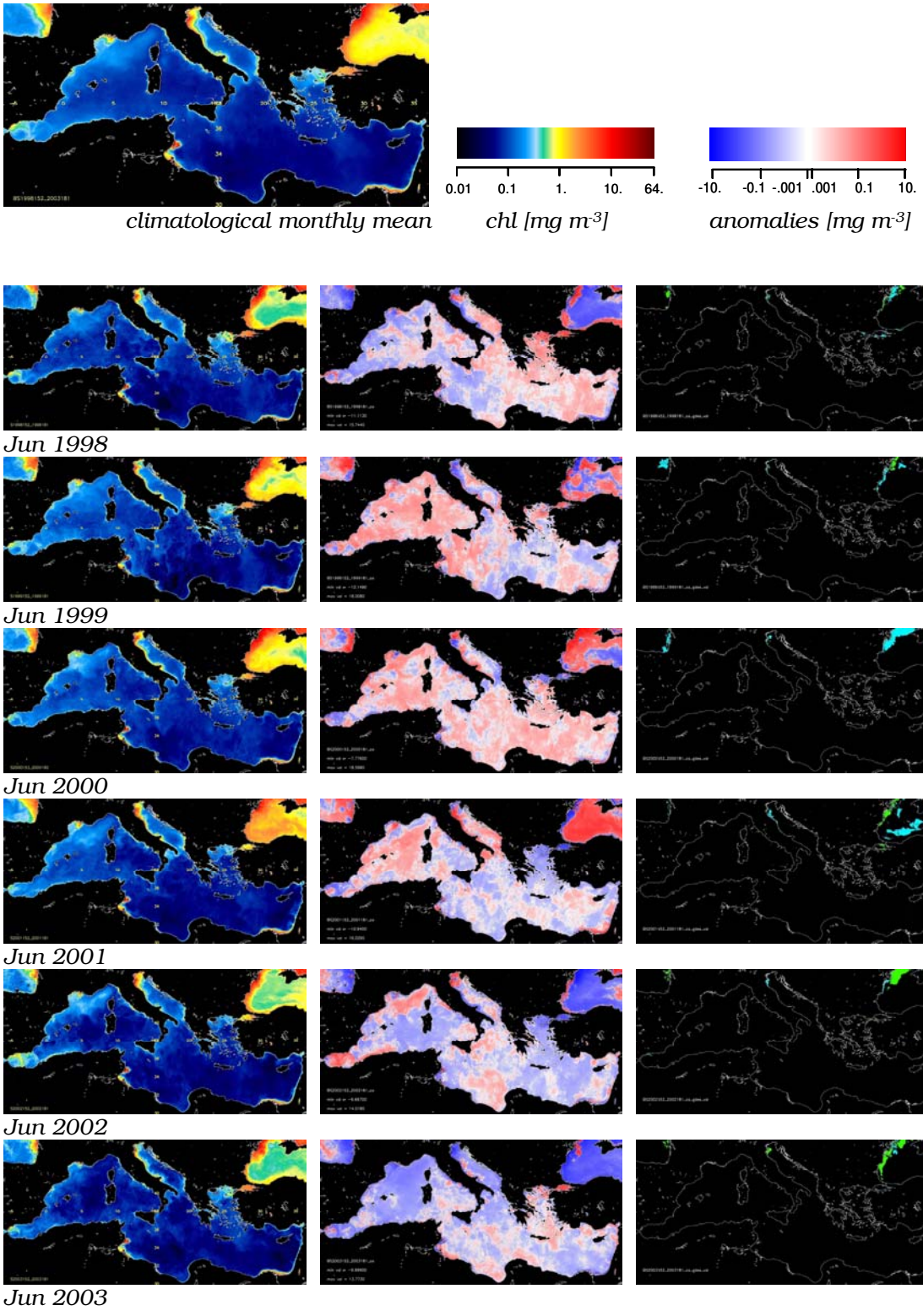

Left panels: monthly mean concentration of chl [mg m^{-3}]
Middle panels: chl anomalies [mg m^{-3}] as mean concentration – climatological value
Right panels: excess anomalies (blue < -1 mg m^{-3}, green > +1 mg m^{-3})

Figure 19. Monthly Anomalies: July

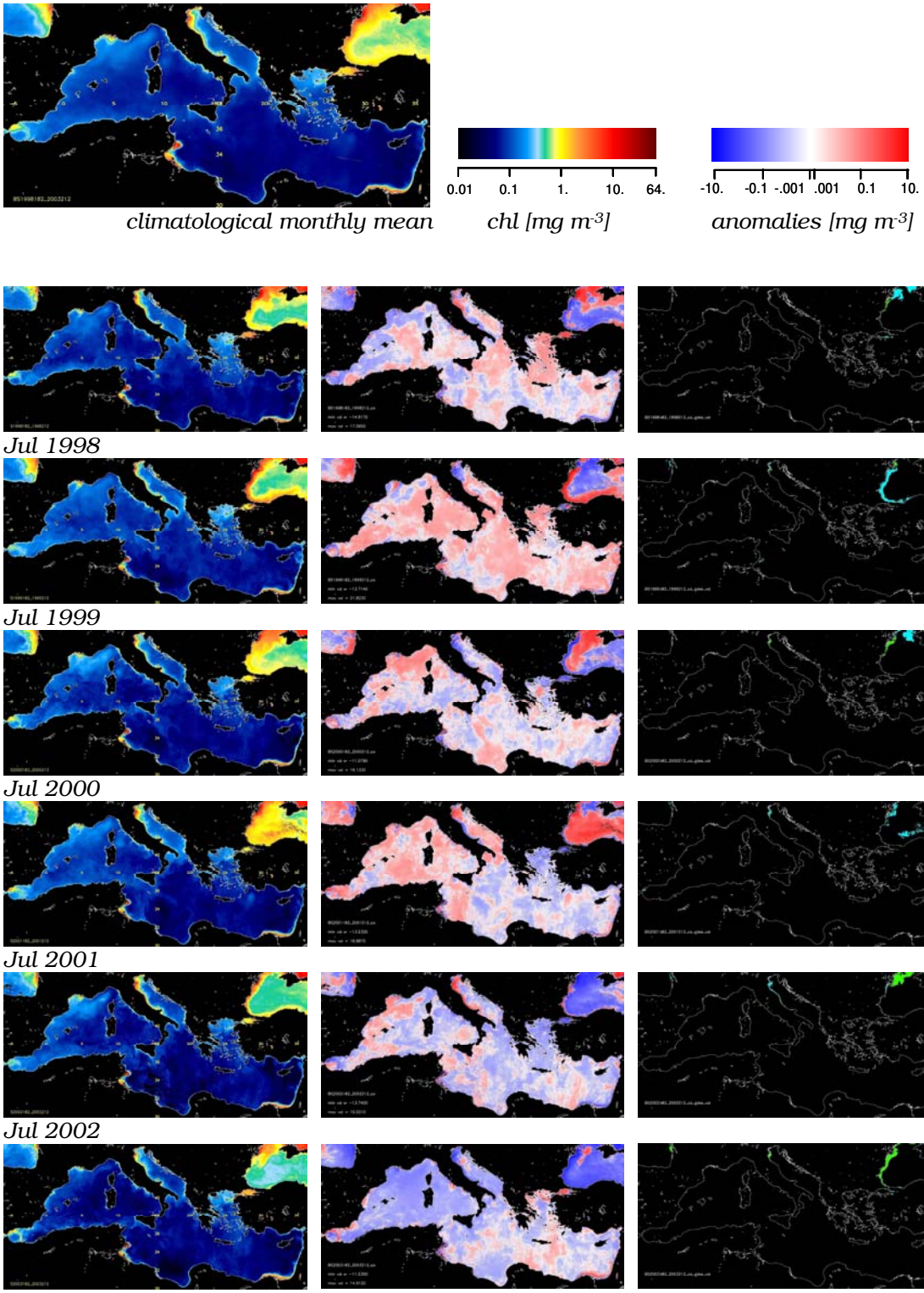

Left panels: monthly mean concentration of chl [mg m^{-3}]
Middle panels: chl anomalies [mg m^{-3}] as mean concentration – climatological value
Right panels: excess anomalies (blue < -1 mg m^{-3}, green > +1 mg m^{-3})

Figure 20. Monthly Anomalies: August

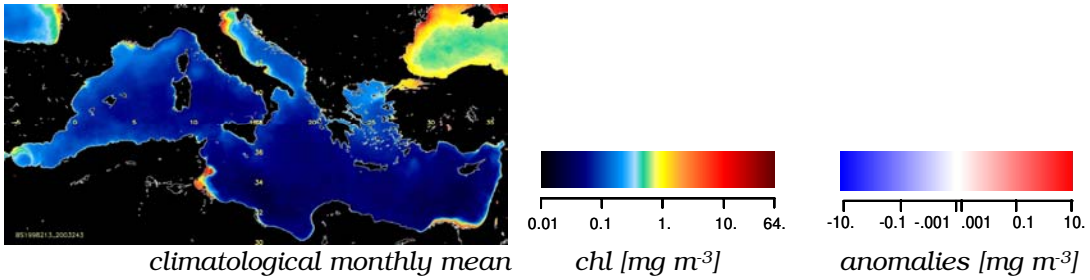

climatological monthly mean *chl [mg m^{-3}]* *anomalies [mg m^{-3}]*

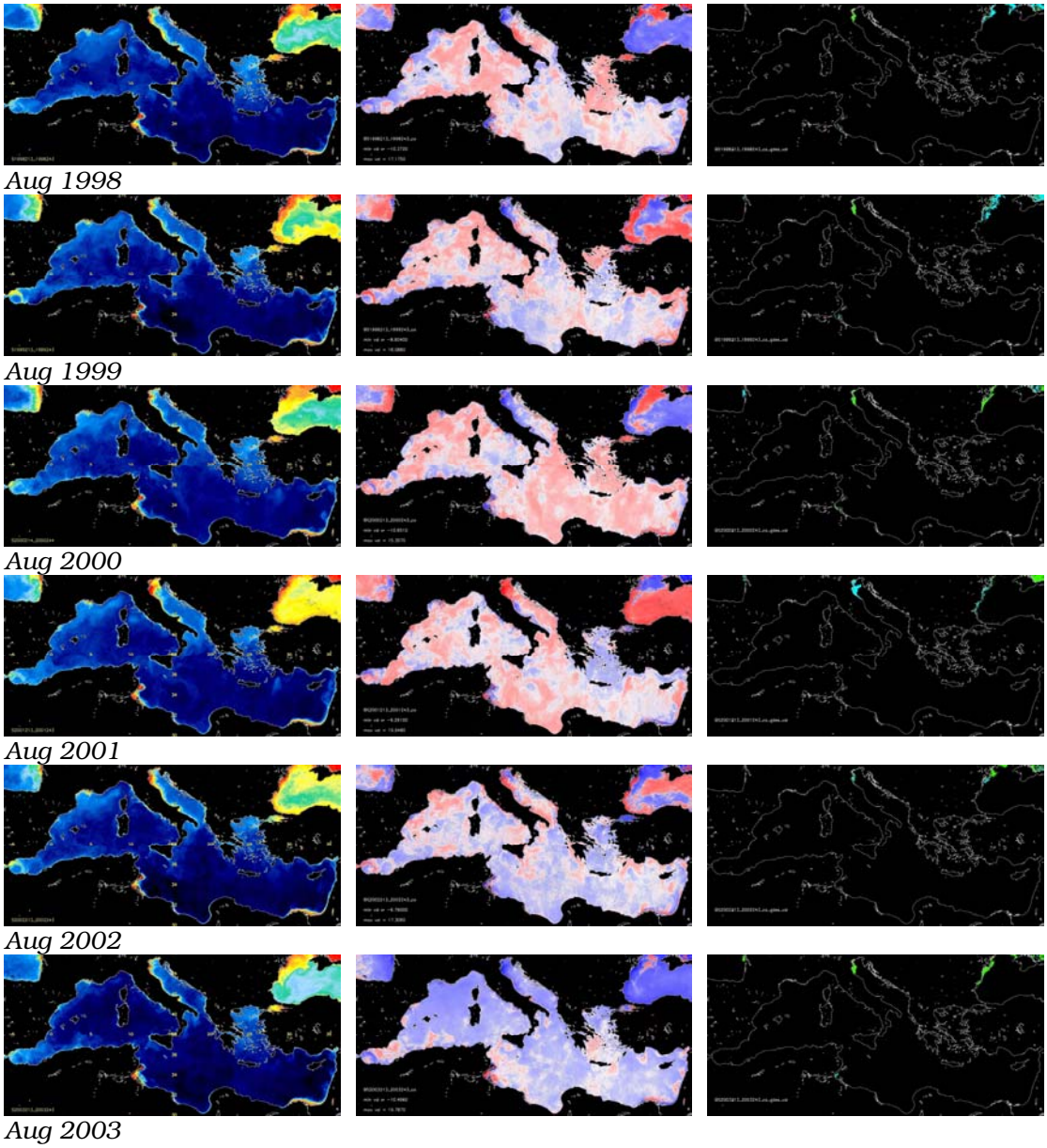

Aug 1998

Aug 1999

Aug 2000

Aug 2001

Aug 2002

Aug 2003

Left panels: monthly mean concentration of chl [mg m^{-3}]
Middle panels: chl anomalies [mg m^{-3}] as mean concentration – climatological value
Right panels: excess anomalies (blue < -1 mg m^{-3}, green > +1 mg m^{-3})

Figure 21. Monthly Anomalies: September

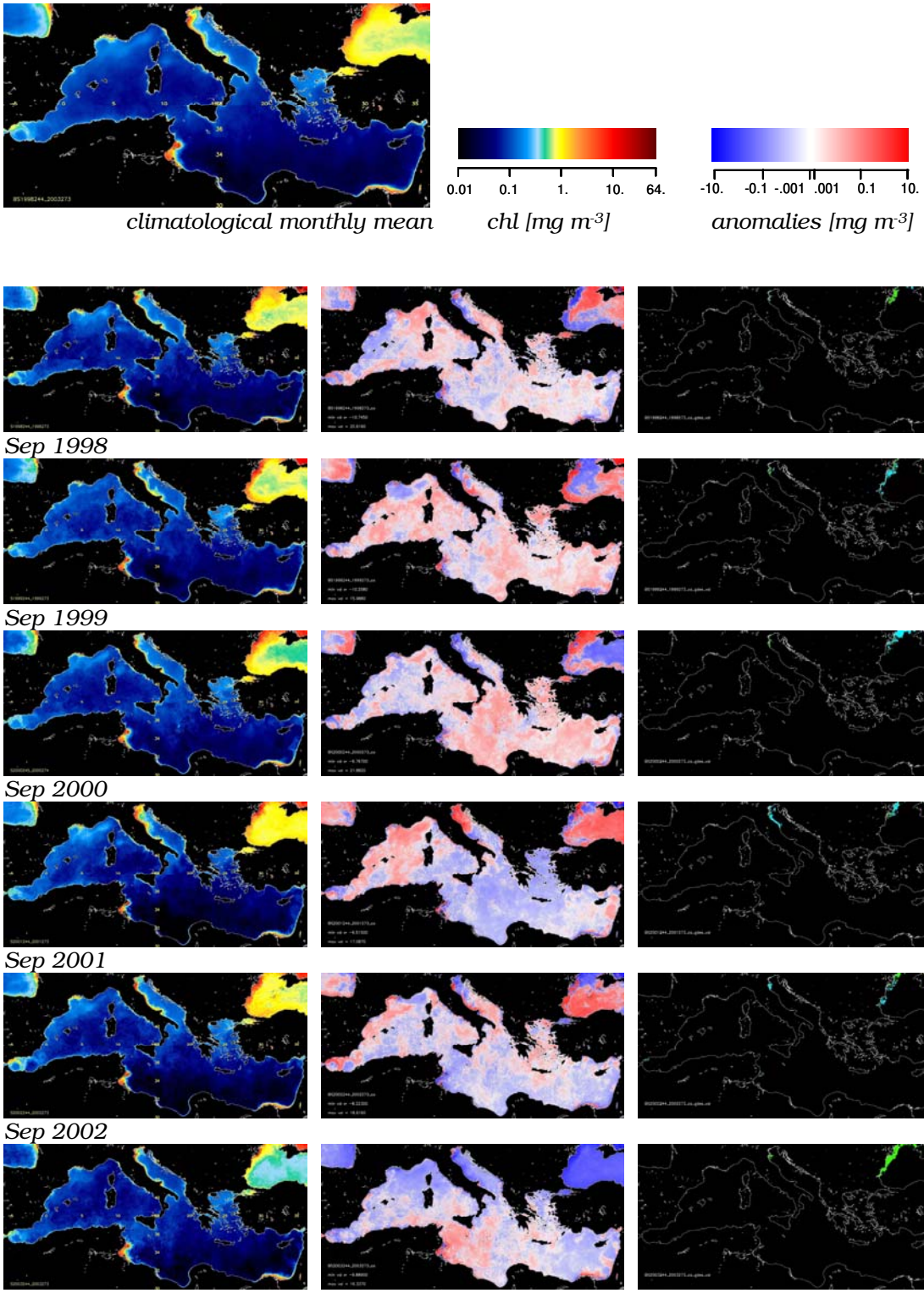

Left panels: monthly mean concentration of chl [mg m^{-3}]
Middle panels: chl anomalies [mg m^{-3}] as mean concentration – climatological value
Right panels: excess anomalies (blue < -1 mg m^{-3}, green > +1 mg m^{-3})

Figure 22. Monthly Anomalies: October

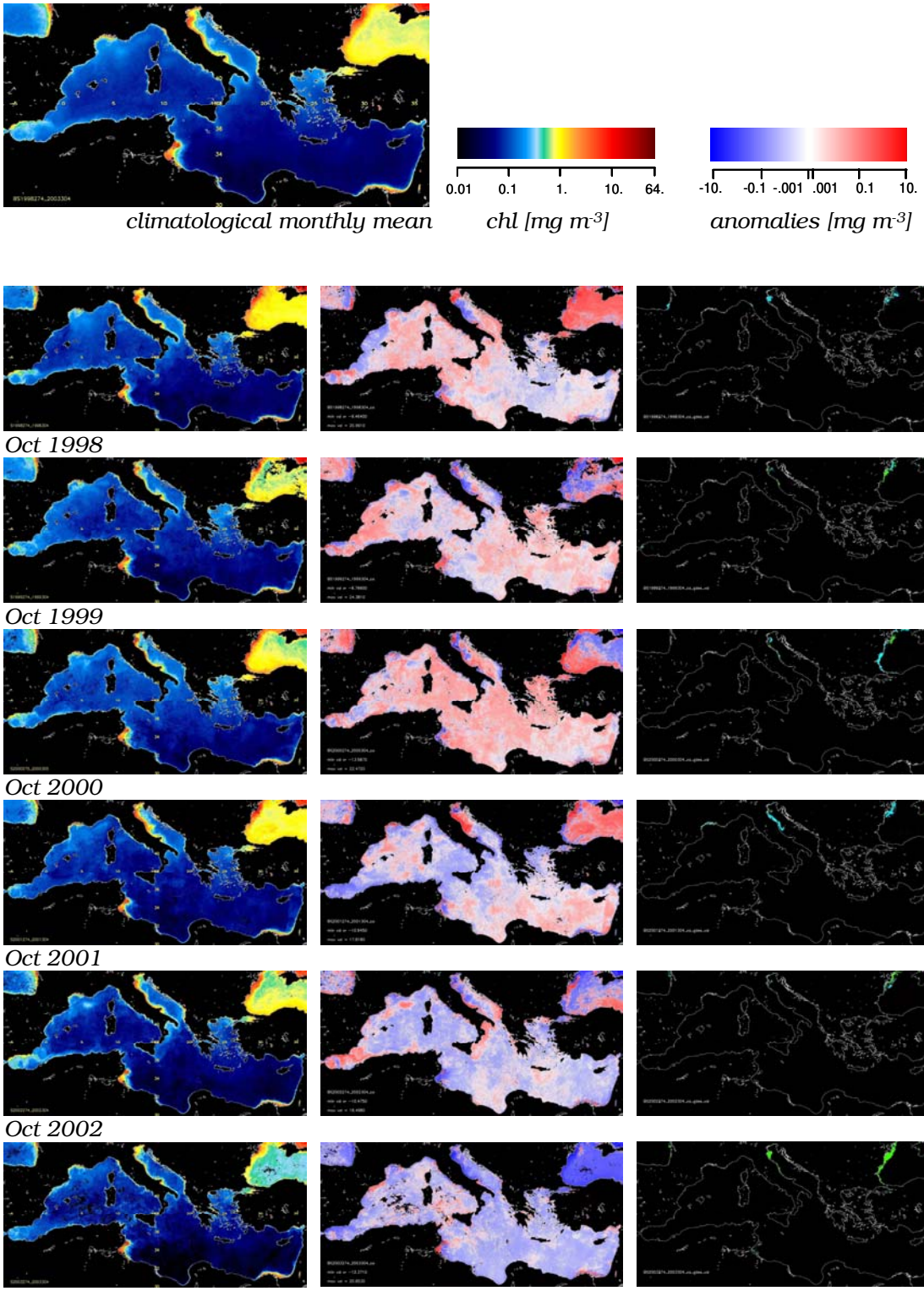

Left panels: monthly mean concentration of chl [mg m^{-3}]
Middle panels: chl anomalies [mg m^{-3}] as mean concentration – climatological value
Right panels: excess anomalies (blue < -1 mg m^{-3}, green > +1 mg m^{-3})

Figure 23. Monthly Anomalies: November

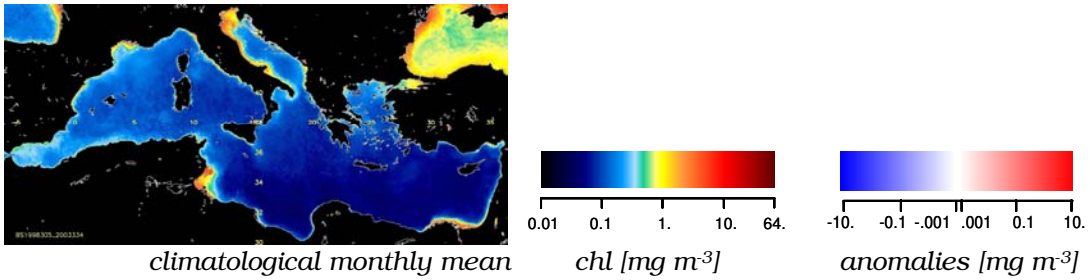

climatological monthly mean *chl [mg m^{-3}]* *anomalies [mg m^{-3}]*

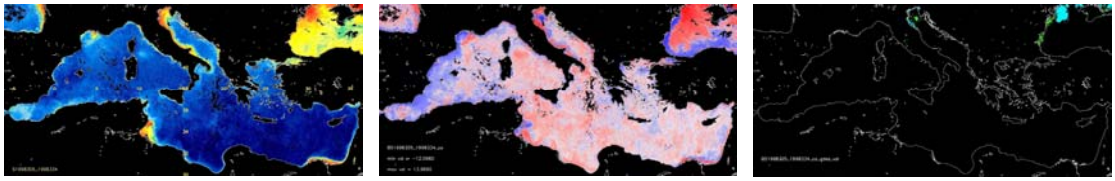

Nov 1998

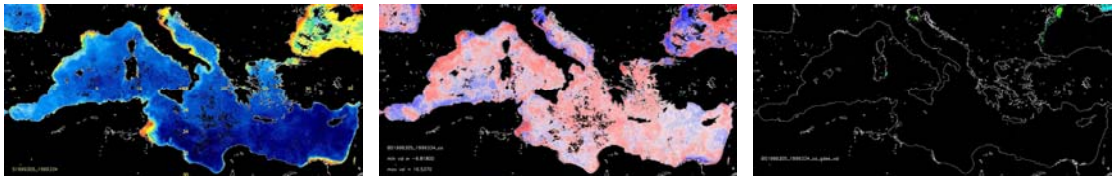

Nov 1999

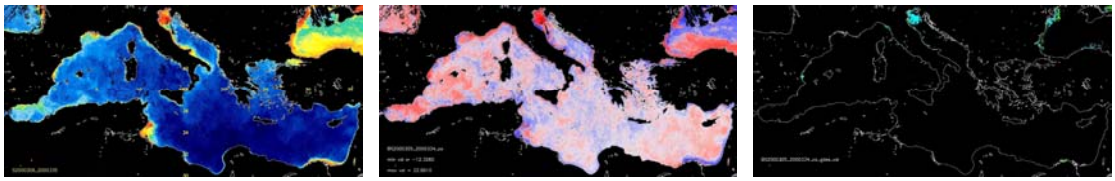

Nov 2000

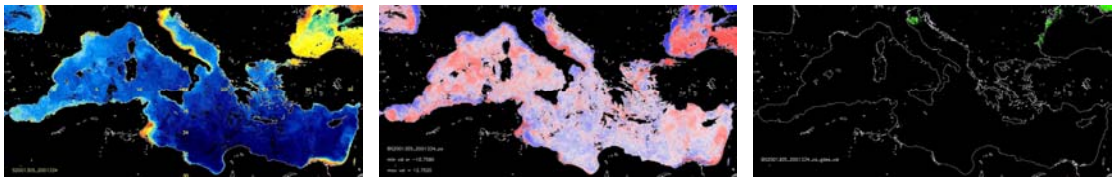

Nov 2001

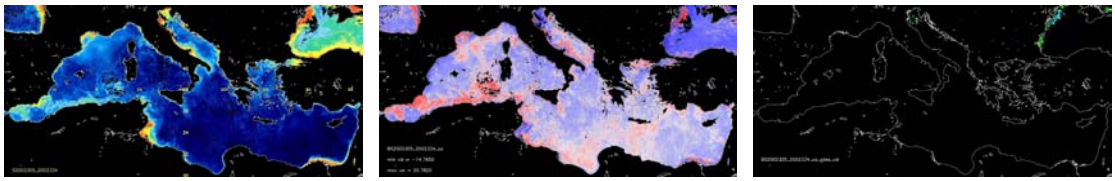

Nov 2002

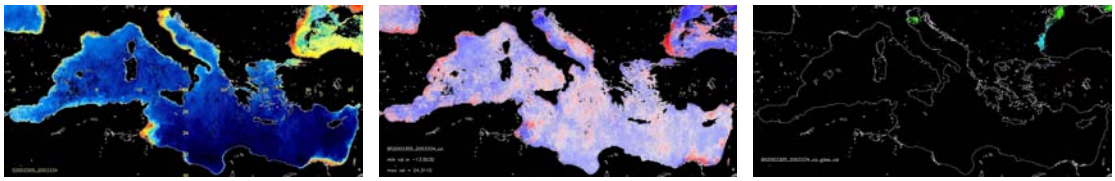

Nov 2003

Left panels: monthly mean concentration of chl [mg m^{-3}]
Middle panels: chl anomalies [mg m^{-3}] as mean concentration – climatological value
Right panels: excess anomalies (blue < -1 mg m^{-3}, green > +1 mg m^{-3})

Figure 24. Monthly Anomalies: December

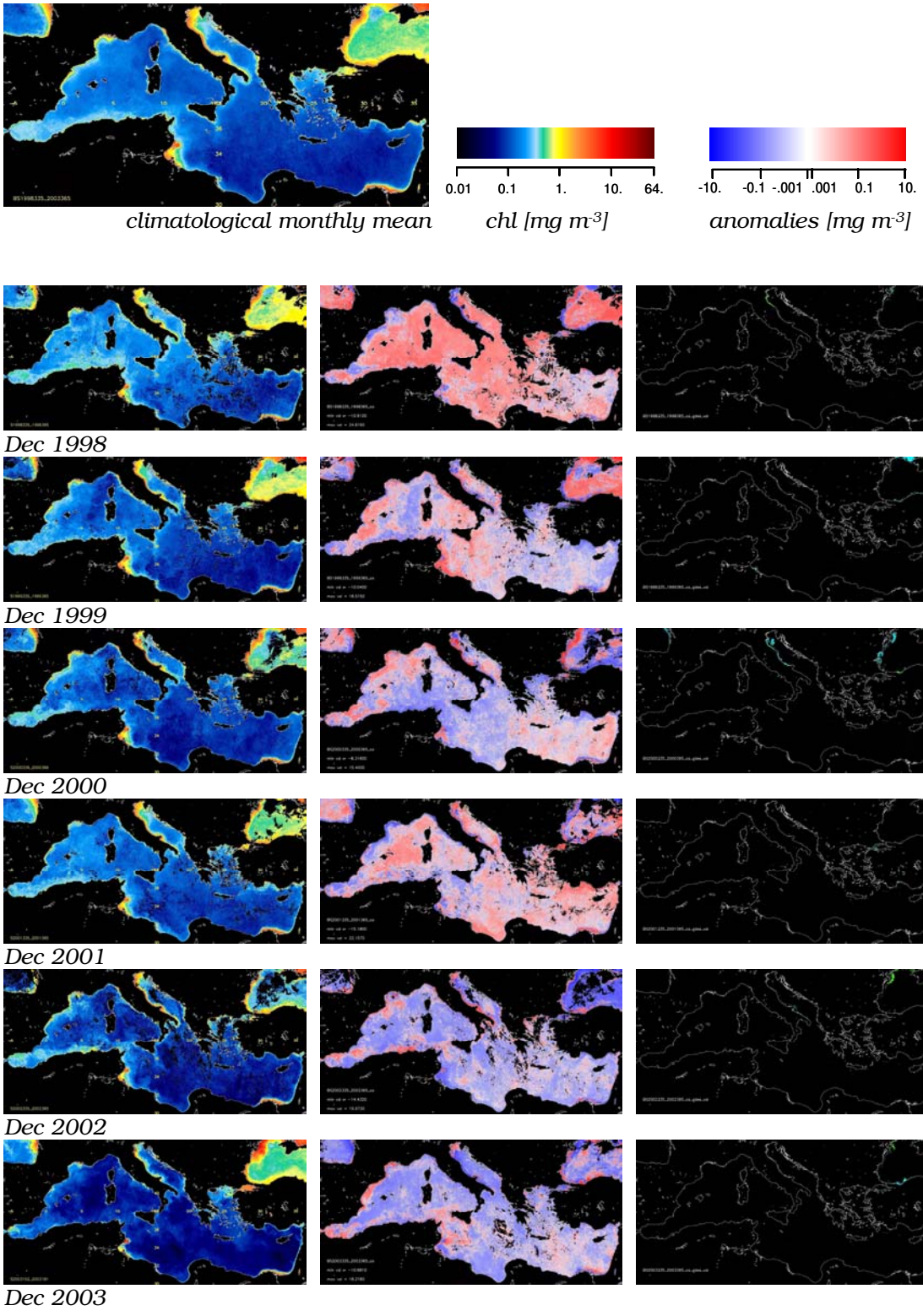

Left panels: monthly mean concentration of chl [mg m^{-3}]
Middle panels: chl anomalies [mg m^{-3}] as mean concentration – climatological value
Right panels: excess anomalies (blue < -1 mg m^{-3}, green > +1 mg m^{-3})

4. Conclusion and Future Activities

The analysis of SeaWiFS-derived *chl* anomalies provides a novel insight into the space and time patterns of biological cycles in the Mediterranean Sea, demonstrating algal blooms dynamics and related environmental boundary conditions. The approach adopted here suggests the hypothesis of a relationship between geographic and climatic factors and bio-geo-chemistry of the basin. The mechanisms of fertilization of the basin, supporting recurrent or anomalous blooming, appear to be ruled mainly by coastal interactions and atmospheric forcing, and then by the ensuing thermohaline dynamics. Therefore, the environmental status of the system would seem to be determined primarily by the key morphological and meteorological features of the basin, upon which may (in near-coastal areas) or may not (in the open sea) be superimposed an anthropogenic impact.

Additional information could be extracted from the data set presented here, by an in-depth analysis of both the *chl* monthly mean record and the sequence of monthly anomalies computed on the basis of the climatological data record. Future activities, in the next phase of the present research program, should include an assessment of the general trend presented by the monthly means, on a pixel-by-pixel basis. Such a trend could be visualized in image form first by computing for each pixel a linear regression of the *chl* values in the monthly means, and then by displaying the value of the fitted line's slope on the same geographical grid used for the composites. Furthermore, histograms of positive anomalies (percent value) should be compiled, at both the yearly and monthly scale. The analysis of such histograms would allow estimating the threshold(s) separating simple recurrent blooms, confined within a certain interval, from exceptional blooms, in which the high *chl* values would represent truly anomalous episodes occurring in response to particular environmental boundary conditions.

Finally, the obvious limitation of a yearly/monthly analysis, in light of potential algal blooms limited to days or weeks, would suggest as appropriate the development of an anomaly assessment technique designed to detect this kind of short-term (albeit also recurring, in principle) events. A "bloom anomaly algorithm" should be devised to detect anomalous *chl* as the difference between the actual (or mean) value measured for a pixel on a given day (or short period, up to the weekly scale, in order to compensate by compositing possible holes in the daily coverage) and the running mean value computed for the same pixel in the period ranging from, say 2 weeks before to 2 weeks after that day (or short period). The application of this assessment technique to the entire SeaWiFS database, for the Mediterranean or other basins, would allow carrying out a systematic comparison of recurrent and anomalous algal blooming events in the European enclosed and marginal seas.

References

Antoine, D., A. Morel and J.M. André (1995). "Algal pigment distribution and primary production in the eastern Mediterranean as derived from Coastal Zone Color Scanner observations". *Journal of Geophysical Research*, vol. 100, p. 16193-16209.

Arnone, R.A., D.A. Wiesenburg and K.D. Saunders (1990). "The origin and characteristics of the Algerian Current". *Journal of Geophysical Research*, vol. 95, p. 1587-1598.

Barale, V. (1994). "Ocean colour, planktonic pigments & productivity". *Memoires de l'Institut Oceanographique, Monaco*, n. 18, p. 23-33.

Barale, V. (2000). "Integrated geographical and environmental remotely-sensed data on marginal and enclosed basins: the Mediterranean case". In: *Marine and Coastal Geographic information Systems*, D. Wright and D. Bartlett ed.s, 'Research Monographs in Geographic Information Systems' series, Taylor & Francis, London, p.177-187.

Barale, V. (2003). "Environmental remote sensing of the Mediterranean Sea". *Journal of Environmental Science and Health,* vol. A38, no. 8, p. 1681-1688.

Barale, V. and D.J. Larkin (1998). "Optical remote sensing of coastal plumes and run-off in the Mediterranean region". *Journal of Coastal Conservation*, vol. 4, p. 51-68.

Barale, V., D. Larkin, L. Fusco, J.M. Melinotte and G. Pittella (1999). "OCEAN Project: the European archive of CZCS historical data". *International Journal of Remote Sensing*, vol. 20 (7), p. 1201-1218.

Barale, V., C.R. McClain and P. Malanotte-Rizzoli (1986). Space and time variability of the surface color field in the northern Adriatic Sea. *Journal of Geophysical Research*, vol. 91, p. 12957-12974.

Barale, V., S. Panigada and M. Zanardelli (2002). "Habitat preferences of fin whales (*Balaenoptera physalus*) in the northwestern Mediterranean Sea: a comparison between in situ and remote sensing data". In: *Proceedings of the 7th Thematic Conference 'Remote Sensing for Marine and Coastal Environments'*, Miami, FL, USA, 20-22 May 2002 (on CD-ROM, VERIDIAN, Ann Arbor, MI, USA, 2002).

Barale, V., and P.M. Schlittenhardt (1994). "Monitoring the marginal seas of Europe with optical observations". In: *Remote Sensing:*

from Research to Operational Applications in the new Europe, R. Vaughan ed., Springer-Verlag, Budapest, p. 293-298.

Barale, V., and I. Zin (2000). "Impact of continental margins in the Mediterranean Sea: hints from the surface colour and temperature historical record". *Journal of Coastal Conservation*, vol. 6, p. 5-14.

Bricaud, A., E. Bosc and D. Antoine (2002). "Algal biomass and sea surface temperature in the Mediterranean basin: intercomparison of data from various satellite sensors and implications for primary production estimates". *Remote Sensing of Environment*, vol. 81, p. 163-178.

Fu, G., K.S. Baith and C.R. McClain (1998). "SeaDAS: The SeaWiFS Data Analysis System". In: Proceedings of the 4th Pacific Ocean Remote Sensing Conference, Qingdao (China), 28-31 July 1998; p. 73-79.

Gitelson, A., A. Karnieli, N. Goldman, Y.Z. Yacobi and M. Mayo (1996). Chlorophyll estimation in the southeastern Mediterranean using CZCS images: adaptation of an algorithm and its validation". *Journal of Marine Systems*, vol. 9, p. 283-290.

Jaquet, J.M., S. Tassan, V. Barale and M. Sarbaji (1999). "Bathymetric and bottom effects on CZCS chlorophyll-like pigment estimation: data from the Kerkennah shelf (Tunisia)". *International Journal of Remote Sensing*, vol. 20 (7), p. 1343-1362.

Melin, F., B. Bulgarelli, N. Gobron, B. Pinty and R. Tacchi (2000). "An integrated tool for SeaWiFS operational processing". European Commission Publication, no. EUR 19576 EN, Ispra (Italy).

Morel, A. and J.M. André (1991). "Pigment distribution and primary production in the western Mediterranean as derived and modeled from Coastal Zone Color Scanner observations". *Journal of Geophysical Research*, vol. 96, p. 12685-12698.

Sturm, B., V. Barale, D. Larkin, J.H. Andersen and M. Turner (1999). "OCEANcode: the complete set of algorithms and models for the level-2 processing of European CZCS historical data". *International Journal of Remote Sensing*, vol. 20 (7), p. 1219-1248.

Sturm, B. and G. Zibordi (2002). "SeaWiFS atmospheric correction by an approximate model and vicarious calibration". *International Journal of Remote Sensing*, vol. 23 (3), p. 489-501.

THETIS Group (1994). "Open ocean deep convection explored in the Mediterranean". *EOS, Transactions, American Geophysical Union*, vol. 75 (19), p. 217-221.

European Commission

EUR 21479 EN – DG Joint Research Centre, Institute (Name of your institute)

Luxembourg: Office for Official Publications of the European Communities
2004– 52 pp. – 21 x 29.7 cm
EUR - Scientific and Technical Research series; ISSN 1018-5593

Mission of the JRC

The mission of the JRC is to provide customer-driven scientific and technical support for the conception, development, implementation and monitoring of EU policies. As a service of the European Commission, the JRC functions as a reference centre of science and technology for the Union. Close to the policy-making process, it serves the common interest of the Member States, while being independent of special interests, whether private or national.